MexXY-OprM/OprA molecular interactions in *Pseudomonas aeruginosa.*

Submitted by

Carla Daniela Noriega Medrano

A Thesis Submitted to the Faculty of Graduate and Postdoctoral Studies of

The University of Manitoba

in partial fulfillment of the requirements of the degree of

Master of Science

Department of Microbiology

University of Manitoba

Winnipeg, Manitoba, Canada

Copyright © 2026

Abstract

In Canada alone, 38% of patients with cystic fibrosis (CF) have experienced *P. aeruginosa* infections, highlighting this organism as a high-priority pathogen for the development of novel antibiotics. A major challenge in treating these infections is the intrinsic resistance to multiple antibiotics of *P. aeruginosa*, where resistance-nodulation-division efflux pumps, such as MexXY, play a central role. MexXY is an efflux pump that, usually, form a functional complex with the outer membrane protein OprM encoded in the *mexAB-oprM* operon; however, in certain strains, it associates instead with OprA, an alternative outer membrane protein encoded within the *mexXY-oprA* operon.

While MexXY paired with OprM primarily confers resistance to aminoglycosides, when MexXY forms the complex with OprA exhibits an expanded substate profile that includes β-lactam antibiotics like sulbenicillin and carbenicillin. Despite structural similarities, OprM and OprA share only 46% amino acid identity, with significant differences located in their α-helical domains. In this work, determinants of substrate selection were studied using chimeric MexXY-OprM/OprA systems, where OprM α-helixes domains were substituted with the corresponding from OprA. Seven chimeric constructs were generated and integrated them into the chromosome of an efflux pump-deficient *P. aeruginosa* strain. Efflux activity was assessed using ethidium bromide susceptibility assays and broth microdilution MIC assays with various antibiotics. Among the seven strains with the chimera efflux pump complex, substitution of the α4 helix exhibited gain of function, restoring sulbenicillin efflux to levels comparable to the MexXY-OprA reference complex.

Given the limited characterization of *mexXY-oprA* operon, its prevalence across *Pseudomonas* species remains unclear. This study screened whole-genome sequences using BLASTn against the RefSeq database to assess the presence of the operon within *Pseudomonas* spp. Phylogenetic relationships were validated through a *rpoB*-based analysis, and the genomic context of the operon was examined through a comparative gene cluster analysis within *Pseudomonas* spp.

Acknowledgements

First, I would like to express my sincere gratitude to my supervisor, Dr. Ayush Kumar, for the opportunity to work in his amazing research lab and his continuous feedback provided during this project. His patience, expertise, and guidance were crucial for the completion of this thesis and to my development as a researcher.

I would also like to thank to my committee members, Dr. Karen Brassinga and Dr. Sean McKenna for their valuable feedback and guidance.

I am deeply grateful to the Kumar Lab members, past and present, for creating a fun and helpful environment that made work enjoyable. Thank you for the many scientific and life discussions, and for always helping me troubleshoot whenever I needed it. A special mention to Elaine, thank you for adopting me as your favorite Mexican and, most importantly, as your friend. Graduate school would not have been the same without you. Words cannot express how much I appreciate having you in my life.

Lastly, I need to thank to my best friend and partner, Nathaniel, your support and understanding during this process were essential to my success. I am deeply grateful for all the kind words, motivation, thoughtful curiosity and genuine effort to understand my work. Thank you for reminding me of my strength and capacity to do give my best every single day.

Dedication

Para mis padres, este trabajo es por y para ustedes. Gracias por siempre creer en mí y apoyarme en cada paso para cumplir mis sueños y metas. Gracias por motivarme a mejorar cada día y por la paciencia y el amor con los que me formaron.

In memory of Sebastian Delgado, all of this started thanks to you. I hope I made you proud.

Table of contents

Contribution of authors

Carla Daniela Noriega Medrano wrote the literature review presented in Chapter I.

The experiments described in Chapter II were designed by Carla Daniela Noriega Medrano and Ayush Kumar. All experimental work was performed by Carla Daniela Noriega Medrano. Data analysis was carried out by Carla Daniela Noriega Medrano and Ayush Kumar.

In Chapter III the bioinformatic analysis and data interpretation were designed by Carla Daniela Noriega Medrano and Ayush Kumar, and carried out by Carla Daniela Noriega Medrano. Data analysis was carried out by Carla Daniela Noriega Medrano and Ayush Kumar.

List of tables

List of figures

List of abbreviations

ABC	ATP-binding cassette
AME	Aminoglycoside-modifying enzyme
Amp	Ampicillin
CA-MHA	Cation-adjusted Muller Hinton agar
CA-MHB	Cation-adjusted Muller Hinton broth
Cb	Carbenicillin
CF	Cystic fibrosis
CFRT	Cystic fibrosis transmembrane conductance regulator
EPS	Extracellular polymeric substances
EtBr	Ethidium bromide
Gm	Gentamicin
HGT	Horizontal gene transfer
IPTG	Isopropyl β-D-1-thiogalactopyranoside
Kan	Kanamycin
LB	Lysogeny broth
LPS	Lipopolysaccharides
MATE	Multidrug and toxic compound extrusion
MDR	Multidrug-resistant
MFP	Membrane-fusion protein
MFS	Major facilitator superfamily
MIC	Minimum inhibitory concentration
OD_{600}	Optical density measured at 600 nm

OMF	Outer membrane factor
OMP	Outer membrane protein
PAP	Periplasmic adaptor protein
PBP	Penicillin-binding protein
PCR	Polymerase chain reaction
pLDDT	Predicted local distance difference test
QS	Quorum sensing
RND	Resistance-nodulation division
SMR	Small multidrug resistance
Suc	Sucrose
Sulb	Sulbenicillin
TCSS	Two-component signaling systems
Tet	Tetracycline
UTI	Urinary tract infection

Chapter I: Literature review

1.1 *Pseudomonas aeruginosa*

Pseudomonas aeruginosa is a Gram-negative, monotrichous, rod-shaped pathogen measuring approximately 1-5 µm in length and 0.5-1.0 µm in width. It was first successfully isolated from a soldier's wound infection bandages in 1882 and described as "*Bacterium aeruginosum*" by Schroeter (Schroeter, 1872). It was reclassified in 1894 by Migula as "*Pseudomonas aeruginosa"* (Letizia et al., 2025; Rudra et al., 2022). This bacterium is characterized by its distinctive color resulting from the combination of the pigments pyocyanin and pyoverdine, giving the colors blue and yellow-green respectively, which defines the species term *aeruginosa* (verdigris: aerūgō in Latin) (Letizia et al., 2025).

P. aeruginosa can be found in several different environments and isolated from a wide range of living organisms including plants, animals and humans (Lister et al., 2009). This flexibility is largely attributed to its metabolic versatility which enables adaptation to poor-nutritional and diverse environmental conditions, the ability to survive in challenging habitats, and persistence in communities and nosocomial settings (Krell & Matilla, 2024; Lister et al., 2009).

The *P. aeruginosa* genome is one of the largest of all known bacterial genomes, ranging from 5.5 to 7 million base pairs (Klockgether et al., 2011). The first complete genome of this species to be sequenced was *P. aeruginosa* PAO1 (Holloway, 1955) with a size of 6.3 million base pairs with a size of 6.3 million base pairs (Stover et al., 2000). It revealed an extensive repertoire of genes involved in regulation, as well as numerous

genes associated with transport systems and enzymes involved in metabolism and substrate uptake (Lund-Palau et al., 2016). These features have made *P. aeruginosa* PAO1 the principal reference for genetic and functional studies within the *Pseudomonas* genus (Letizia et al., 2025).

The genomic complexity of *P. aeruginosa* is closely related to its extensive arsenal of cell-associated and extracellular virulence factors. Among the most notable are the single polar flagellum, which enables motility across solid surfaces and within aqueous or low-viscosity environments; the cell surface pili, which facilitate adhesion to host cell membranes and other surfaces; and the ability to form biofilms, which is considered important for *P. aeruginosa* long-term colonization in lung infections (Driscoll et al., 2007; Rossi et al., 2020).

Additional virulence mechanisms include quorum sensing (QS) communication systems and the secretion of exoenzymes that contribute to host altered immune responses and tissue damage (Jurado-Martín et al., 2021).

Together with its diverse virulence mechanisms, *P. aeruginosa* displays a high level of intrinsic antibiotic resistance that will be discussed in more detail in section 1.3.

1.2 Clinical significance of *P. aeruginosa*

Hospitalized patients may be colonized by *P. aeruginosa* upon admission or during their hospitalization owing to the bacterium's ability to survive on a wide range of surfaces within hospital environments. Infections caused by *P. aeruginosa* include, but are not limited to, otitis externa, skin and soft tissue infections, pneumonias, urinary tract infections (UTI's) and blood stream infections (Driscoll et al., 2007). Although it rarely

causes infections in healthy individuals, it can lead to both acute and chronic infections in immunocompromised patients. In particular, patients with cystic fibrosis (CF) commonly experience chronic sinopulmonary colonization and recurrent infections by this pathogen (Letizia et al., 2025).

CF is a genetic disorder caused by mutations in the *CFTR* gene which encodes the CF transmembrane conductance regulator (CFTR), an anion channel regulated by ATP hydrolysis and phosphorylation (Riordan, 2005). Defective or absent CFTR protein function disrupts transepithelial ion homeostasis (Ludovico et al., 2022), leading to airway surface dehydration causing the accumulation of thick and viscous mucous in the respiratory tract of affected individuals (Hansen & Skov, 2015; Oakland et al., 2012). This altered environment provides optimal conditions for bacterial colonization by microbes such as *P. aeruginosa* and *S. aureus* (Castellani & Assael, 2016).

According to the 2023 Canadian Cystic Fibrosis Registry annual report, more than 4,000 Canadians live with cystic fibrosis and 25.6% have experienced an infection by *P. aeruginosa*, making it the most common infection in the adult CF population (Cystic Fibrosis Canada, 2024). Given these characteristics and the significant antibiotic resistance of *P. aeruginosa*, this bacterium has been identified by the World Health Organization as one of the primary high-priority pathogens necessitating urgent development of new antibiotics (World Health Organization, 2024).

1.3 Multidrug resistance mechanisms

The discovery of antibiotics revolutionized the treatment of bacterial infections, particularly in developed countries. However, the widespread and inappropriate use of

antimicrobial agents has accelerated bacterial adaptation leading to the emergence of resistant bacterial strains (Habboush & Guzman, 2023). Antibiotic resistance refers to the ability of bacteria to withstand the effects of a drug specifically designed to eliminate them (CDC, 2025).

Bacterial resistance mechanisms are commonly classified into three categories: intrinsic (or innate), acquired and adaptive. Intrinsic resistance is the simplest type of resistance and is the natural lack of susceptibility to a certain group or groups of antibiotics which may be related to the absence of a receptor for the antibiotic, low affinity, cell wall impermeability or inactivating enzyme production (Urban-Chmiel et al., 2022). Acquired resistance arises from the horizontal transfer of resistance genes or spontaneous mutations that confer new resistant traits. Adaptive resistance involves a reversible or temporary increase in resistance triggered by specific environmental cues or antibiotic exposure. In *P. aeruginosa*, this final mechanism is frequently associated with biofilm formation (Letizia et al., 2025; Pang et al., 2019). The synergy of these resistance mechanisms contributes to the emergence of multidrug-resistant (MDR) strains.

1.3.1 Acquired resistance

Acquired antibiotic resistance in *P. aeruginosa* involves several mechanisms that enable the bacterium to evade the activity of antibiotics. These mechanisms include the overproduction of β-lactamase enzymes, alterations in porin expression or structure, efflux pump overexpression caused by regulatory mutations and modifications in antibiotic targets. Mutations in genes encoding amidases, penicillin-binding proteins (PBPs), lytic transglycosylases, or NuoN (NADH dehydrogenase I chain N) have been shown to enhance *ampC* expression, resulting in the overproduction of cephalosporinase

AmpC responsible for breaking down β-lactam antibiotics (Ropy et al., 2015). Porins such as OprD create channels within the membrane for the uptake of hydrophilic antibiotics; therefore, mutations that alter their expression or function reduce significantly membrane permeability and hence limit antibiotic entry into the cell. Similarly, when efflux pump regulatory genes, such as *mexR, nalB, nalC, nalD or mexZ,* are mutated, overexpression of efflux pumps results (Pang et al., 2019). Another important mutation-driven mechanism of *P. aeruginosa* is the modification of antibiotic targets; mutation in in *gyrA* and *gyrB* (DNA gyrase) or *parC* and *parE* (topoisomerase IV) reduce quinolone binding and thereby decrease susceptibility (Elfadadny et al., 2024).

In addition to mutation-driven mechanisms, *P. aeruginosa* can also acquire antibiotic resistance through horizontal gene transfer (HGT), the process by which genetic information is exchanged between organisms independent of cell division. HGT occurs through three major mechanisms: transformation, where bacteria take up DNA from their environment; transduction, where bacteriophages mediate the transfer of genes between cells; and conjugation, where direct cell-to-cell contact enables the transfer of plasmids or other mobile genetic elements (Burmeister, 2015).

1.3.2 Adaptive resistance

Adaptive resistance can be defined as a temporary increase in the ability of bacteria to withstand antibiotics, induced by environmental stimuli such as the presence of antibiotics. Unlike acquired resistance mechanisms, adaptive resistance is not permanent and become inactive upon removal of the stress factor (Moradali et al., 2017).

Adaptive resistance is frequently mediated by regulatory pathways that modulate gene expression, leading to changes in protein production or target modification. These mechanisms include two-component signaling systems (TCSS), upregulation of the MexXY efflux system, and quorum sensing–dependent biofilm formation (Langendonk et al., 2021).

QS is the intercellular communication system that enables bacteria to detect and respond to extracellular signaling molecules known as autoinducers. This regulatory network coordinates gene expression in a population-density-dependant manner which enables bacteria to express genes that are most beneficial when carried out collectively by the bacterial population acting in synchrony (Rutherford & Bassler, 2012). Up to 10% of the *P. aeruginosa* genome is controlled by QS (Schuster & Greenberg, 2006). Virulence factors under QS control include elastase, proteases, pyocyanin, lectin, rhamnolipids and various toxins, as well as swarming motility and biofilm development (Miranda et al., 2022).

Within the biofilm, bacterial cells are encapsulated within a matrix of extracellular polymeric substances (EPSs) composed of exopolysaccharides, proteins, and DNA, the production of which is triggered by environmental signals such as temperature, pH and nutrient availability, enabling cells firm attachment to surfaces. This mechanism provides several clinical advantages to *P. aeruginosa.* The EPS matrix confers physical protection from the host immune system and acts as a barrier that limits antibiotic penetration to the cells, increasing antimicrobial tolerance. Biofilms also increase water retention which helps the bacteria to survive in hostile environments (Costa et al., 2018). In addition, the

matrix facilitates nutrient absorption and storage; alongside this, it facilitates the adhesion promoting persistent colonization (Elfadadny et al., 2024).

1.3.3 Intrinsic resistance

As in several other Gram-negative bacteria, *P. aeruginosa*'s intrinsic resistance derives primarily from two features. First, its outer membrane exhibits extremely low permeability, estimated to be 12-100 times lower than *E. coli*, because agents that disrupt or permeabilize the outer membrane markedly increase susceptibility to antibiotics. The low permeability limits antibiotic uptake and slows intracellular accumulation, thereby allowing secondary mechanisms, such as energy dependant efflux pumps, to work more efficiently (Hancock & Speert, 2000).

The outer membrane, described as a "molecular sieve", is an asymmetric bilayer of phospholipid and lipopolysaccharides (LPS) containing β-barrel protein channels called porins. This water-filled channels facilitate the entry of most hydrophilic molecules by size. The major porins of *Pseudomonas aeruginosa*, OprF, OprD and OprB, typically form very small-diameter channels, which substantially reduces the diffusion of larger hydrophilic molecules, including antibiotics, into the cell (Breidenstein et al., 2011). Generally, porins are divided into four classes: non-specific porins, such as OprF, which allow the diffusion of small hydrophilic molecules; specific porins, such as OprB, OprD, OprE, OprO and OprP, that allow penetration of particular molecules by specific binding-sites; gated porins, like OprC and OprH, that regulate the uptake of ion complexes; and efflux porins, like OprM, OprN and OprJ, which are important components of efflux pumps (Hancock & Brinkman, 2002).

In addition to reduced outer membrane permeability, the active export of antibiotics via efflux pumps constitutes a major intrinsic resistance mechanism in *P. aeruginosa.* Efflux pumps constitute approximately 6-18% of all membrane transporters in bacterial cells and are currently classified into five superfamilies: the major facilitator superfamily (MFS), the small multidrug resistance (SMR) protein family, the ATP-binding cassette (ABC) family, the resistance-nodulation-division (RND) family, and the multidrug and toxic compound extrusion (MATE) family (Poole & Srikumar, 2001).

Together, these characteristics highlight the central role of efflux systems in shaping *P. aeruginosa*'s intrinsic antibiotic resistance. Among these, the RND family is particularly important, as it mediates the export of a broad range of clinically-relevant antibiotics and are the only pumps that exist in a complex that goes through the outer and inner membrane of the cell (Nikaido, 2011).

1.4 RND efflux pumps

RND efflux systems involve a three-component efflux complex formed by RND-pump protein located in the inner membrane, responsible for molecule transport; a membrane-fusion protein (MFP) or periplasmic adaptor protein (PAP), fixed in the inner membrane and whose role is to stabilize the whole complex, belonging to the membrane fusion protein family; and the outer membrane channel protein (OMP) belonging to the outer membrane factor (OMF) family (Hancock & Brinkman, 2002; Nikaido, 2011; Phan et al., 2015).

The first example of an RND pump with multidrug exporter function was identified in 1993 as AcrB in *E. coli* (Ma et al., 1993), with the AcrAB-TolC complex being one of the

best studied members of these pumps (along with MexAB-OprM from *P. aeruginosa*), and known for expelling diverse molecules as antibiotics, heavy metals, dyes, detergents and solvents (Kumar & Schweizer, 2005). However, RND exporters show selectivity in their transport function, avoiding non-specific binding to essential nutrients or non-toxic metabolites as carbohydrates, amino acids nucleotides, vitamins and minerals (Avakh et al., 2023).

Twelve RND pump encoding operons have been identified in *P. aeruginosa*: *mexAB-oprM, mexCD-oprJ, mexEF-oprN, mexGHI-opmD, mexJK-oprM, mexMN-oprM, mexPQ-opmE, mexVW-opM, mexXY-oprM, muxABC-opmB, triABC-OpmH,* and the mobilizable *tmexCD-topJ* gene cluster (Aendekerk et al., 2002; Chuanchuen et al., 2002; Dong et al., 2022; Köhler et al., 1997; Y. Li et al., 2003; Mima et al., 2005, 2007, 2009; Mine et al., 1999; Poole et al., 1993, 1996). Four of these efflux pumps have been studied extensively due to their contribution to MDR — MexAB-OprM, MexXY, MexEF-OprN, and MexCD-OprJ.

RND efflux pumps exhibit a wide range of substrate specificity, ranging from narrowly selective systems that transport single compounds to multidrug pumps capable of effluxing a wide spectrum of diverse compounds. MexAB-OprM actively expels several classes of antibiotics, including fluoroquinolones, β-lactams, macrolides, lincomycin and others. In contrast, MexXY-OprM, despite sharing a partially overlapping substrate profile to MexAB-OprM, plays a dominant role in aminoglycoside resistance, acting in synergy with aminoglycoside-modifying enzymes (AME's) (Avakh et al., 2023). This system is particularly relevant in *P. aeruginosa* CF isolates, where loss or reduced expression of the MexB component compromises MexAB-OprM functionality, leading to compensatory

overexpression of MexXY-OprM, which partially assumes the efflux role normally fulfilled by MexAB-OprM (Vettoretti et al., 2009).

1.4.1 Substrate transport mechanism

RND efflux pumps mediate substrate extrusion through a proton motive force-driven mechanism that couples inner membrane transport to direct export across the outer membrane. These tripartite systems form a continuous channel spanning the periplasm, enabling the translocation of structurally diverse compounds from the cytoplasm or periplasm to the extracellular environment.

Insight into the molecular basis of substrate transport was provided by the crystal structure of the RND-pump protein AcrB with bonding substrates (Murakami, 2016). The structure revealed an asymmetric homotrimer in which each protomer adopts a different conformational state leading to the proposal of a functional rotation mechanism. In this model, the three protomers cycle sequentially through “access”, “binding” and “extrusion” conformations, enabling continuous substrate transport.

In the cytoplasmatic domain of each protomer, which projects into the periplasmic space, charged residues protonation and deprotonation in the transmembrane helixes trigger molecular motion transmitted to the periplasmic domain causing substrate translocation. During the “binding” state, protomers form spacious pockets in the porter domain to accommodate substrate binding, whereas in the “extrusion” state, the pocket gets shrunken without space to accommodate substrates expelling them toward the outer membrane channel (Murakami et al., 2006).

At the top of the periplasmic region lies the TolC-docking domain, which mediates the interaction with the PAP and OMP in the assembled tripartite complex. Although movement in this region is not commonly observed, it is thought that structural changes may occur moving the whole tripartite complex (Murakami, 2016).

In addition to conformational changes within the RND-pump protein, the outer membrane protein also contributes to substance extrusion. Proteins such as OprM, are proposed to undergo an open/close mechanism that extends to the periplasm to permit substrate release (Phan et al., 2010).

1.4.2 Outer membrane factors

In general, OMFs are homotrimeric proteins that assemble into elongated, tubular channels, with one end embedded in the outer membrane and the opposite end extending into the periplasm where it interacts with the peptidoglycan layer. Despite their low overall sequence identity, OMFs share a highly conserved structural architecture (Alav et al., 2021). Representative members of the OMF family include TolC (*E. coli*), OprM (*P. aeruginosa*) and VceC (*Vibrio cholerae*).

TolC is a well-characterized OMP of the AcrAB-TolC RND efflux complex in *E. coli*. It assembles as a trimer composed of a 40 Å long β-barrel domain embedded in the outer membrane and a 100 Å long α-helical domain formed by 12 coiled coils (4 from each monomer) extending into the periplasm (Blair & Piddock, 2009). This architecture creates a large, water-filled channel of approximately 43,000 $Å^3$, enabling the transport of large substrates and forming a continuous channel through which molecules, including antibiotics, are expelled from the cell (Masi & Pagès, 2013). Studies suggest that TolC is

recruited only after AcrA and AcrB associate forming a sealed complex that allows the substrates to pass directly from AcrB to TolC without leakage into the periplasm, indicating a well-coordinated interaction among the three components (Symmons et al., 2009).

Notably, the assembly of some RND efflux complexes is influenced by substrate availability. In the presence of triclosan, MexJK forms a functional complex with OmpH, whereas in the presence of erythromycin it preferentially associates with OprM (Chuanchuen et al., 2002). This substrate-dependent assembly highlights the functional interchangeability of OMPs within certain efflux systems. Consistent with this flexibility, only six efflux pump operons encode to their own OMP gene and instead rely on the OMPs expressed elsewhere in the genome (Huang et al., 2013; A. Kumar & Schweizer, 2005). One example is the *mexXY* operon expressed in *P. aeruginosa*, which lacks an OMP coding sequence but forms a functional complex in collaboration with OprM from the *mexAB-oprM* operon (Mine et al., 1999).

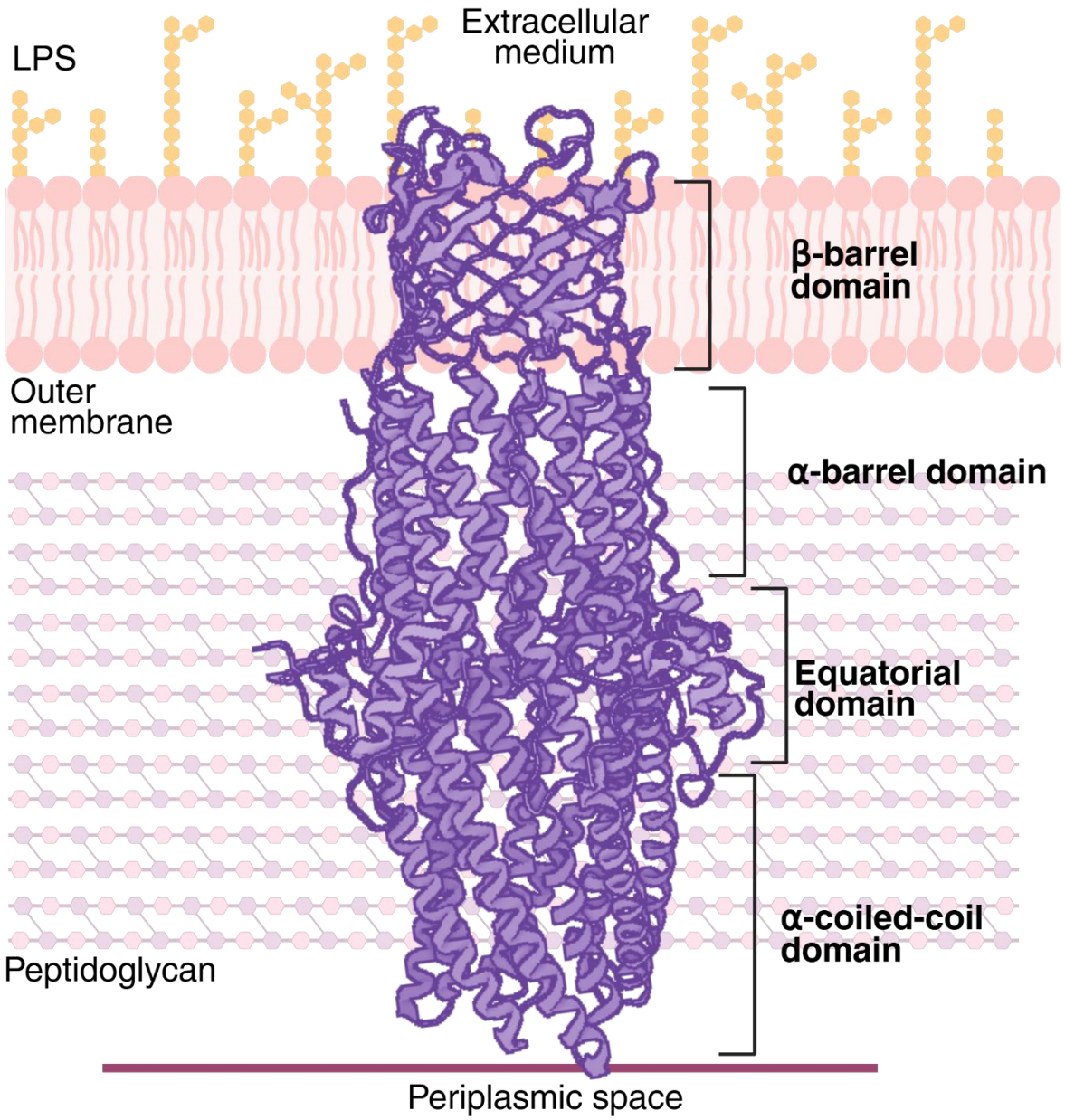

Figure 1 OMP general structure. Ribbon representation of an outer membrane protein constituted α- and β-barrel domains. α domain is divided into three subdomains: α-barrel, equatorial and coiled-coil.

Given the central role of OMPs in determining efflux efficiency and substrate specificity, particular attention has been focused on OprM and OprA in *Pseudomonas spp.* While OprM is the canonical OMP associated with multiple RND efflux systems in *P. aeruginosa*, including MexAB and MexXY, certain strains encode alternative OMPs that can functionally substitute for OprM.

One such example is *P. (para)aeruginosa* PA7, where the *mexXY* operon includes the OMP-coding gene *oprA* (Déraspe et al., 2025; Roy et al., 2010). Comparative studies made with MexXY-OprM and MexXY-OprA have shown that, although both systems share largely overlapping substrate specificities, they differ in efflux efficiency for specific antibiotic classes. In particular, the MexXY-OprA complex from PA7 exhibits enhanced extrusion of β-lactam antibiotics, such as sulbenicillin and carbenicillin, in addition to aminoglycosides, whereas MexXY-OprM appears to be limited to aminoglycoside extrusion (Avakh et al., 2023; Singh et al., 2020).

Despite their functional relatedness, OprM and OprA substantially diverge at amino acid level, sharing only 44% identity and 55% similarity (Morita et al., 2012b). This divergence suggests that subtle structural differences within the OMP channel may influence substrate recognition, channel gating or interaction with the MexXY transporter, contributing to the observed differences in efflux performance.

1.5 Prevalence and Evolution of *oprA* in *Pseudomonas Species*

As mentioned previously, the *mexXY* operon in the *P. aeruginosa* PAO1 strain does not encode an OMP and instead forms a functional efflux complex through association with OprM, which is encoded by a separate operon. In contrast, *P. aeruginosa* strain

PA7—reclassified as *P. paraeruginosa* in 2022 (Rudra et al., 2022)—contains the *oprA* gene within the *mexXY* operon.

Comparative analyses of OprA from PA7 with OprM from PAO1, TolC from *E. coli*, OprA from *Burkholderia* spp., OprZ from *Achromobacter xylosoxidans*, and AdeC from *Acinetobacter baumannii* revealed that OprA shares greater sequence similarity with OMPs from certain *Burkholderia* species than with other *Pseudomonas* OMPs. Notably, a 72–amino acid region located downstream of MexY in PAO1 exhibited strong similarity to the N-terminal region of OprA from PA7 (Morita et al., 2012b).

These observations suggest that ancestral *P. aeruginosa* strains may have possessed a *mexXY–oprA* locus, which was subsequently lost or pseudogenized in PAO1-like lineages. Strains carrying a disrupted or nonfunctional *oprA* gene may have become more prevalent over time, leading to the current distribution observed among *Pseudomonas* spp. (Morita et al., 2012a).

Collectively, these findings indicate that *oprA* is not broadly conserved across *Pseudomonas* spp. but instead exhibits a strain- and lineage-specific distribution, suggesting that selective pressures have favored either the retention or loss of this OMP depending on ecological and clinical contexts.

1.6 Research rationale

Studies comparing MexXY-OprM and MexXY-OprA have shown that, though both complexes share overlapping substrate profiles, the MexXY-OprA complex from *P. aeruginosa* PA7 displays enhanced efflux of antibiotics such as sulbenicillin and carbenicillin in addition to aminoglycosides, whereas MexXY-OprM that is limited to aminoglycoside extrusion (Avakh et al., 2023; Singh et al., 2020). Despite their functional similarity, OprA and OprM share only 44% amino acid identity (Morita et al., 2012b) with the greatest divergence located in the α-helical regions. Accordingly, this study focuses on targeting α-helical regions of OprM to identify residues that influence substrate specificity of the MexXY efflux pump. These regions are of particular interest because the α-helical domain of OMP proteins mediates interactions with the membrane fusion protein (MFP) component of the complex (Du et al., 2014), and mutations within this domain of OprM have been shown to alter MFP binding (Nehme & Poole, 2007). The homologous efflux pump complex, AcrAB-TolC, suggests that α-helical regions in the OMP not only have influence on the interaction between the periplasmatic adaptor protein and the outer membrane protein through the coiled structures, but also have a high structural importance which could contribute to the substrate specificity in the MexXY complex with OprM and OprA outer membrane proteins (Koronakis et al., 2000). With this project, we aim to identify OprM domains critical for interaction with MexXY and formation of a functional efflux complex.

1.7 Hypothesis and research objectives

We hypothesized that α-helix structures in the outer membrane protein (OMP) play a key role in the substrate selectivity of the MexXY-OprM/OprA efflux pump complex.

Objectives:

1. Elucidate the molecular interactions between the three components of the efflux pump MexXY-OprM/OprA.

2. To identify the prevalence of *mexXY-oprA* operon in *Pseudomonas* spp.

Chapter II: α-helix structure role in OMP substrate selection: OprM vs. OprA in *P. aeruginosa*

2.1 Materials and methods

2.1.1 Oligonucleotides, plasmids, bacterial strains and growth conditions

All the bacterial strains, plasmids and oligonucleotides used in this study are listed in Table 1, Table 2 and Table 3, respectively. All strains were grown in LB broth Lennox (BD Difco) medium at 37°C with shaking at 225 rpm. Bacterial cells were also grown on LB agar at 37°C regularly.

Antibiotics and selection compounds were added to the LB media as necessary at the following concentrations: gentamicin (Gm) 15 µg/mL for *E. coli*, 30 µg/mL for *P. aeruginosa*, carbenicillin (Cb) 200 µg/mL, ampicillin (Amp) 100 µg/mL, sucrose (Suc) 5% (w/v). For gene expression induction in *P. aeruginosa,* media was supplemented with 1 mM of isopropyl β-D-1-thiogalactopyranoside (IPTG).

2.1.2 Construction of chimeric OMP operon, cloning and genetic manipulation of *P. aeruginosa*

Seven OMP *oprM/oprA* chimera gene sequences were designed from the genome sequence of *P. aeruginosa* PA7 (GeneBank ID: CP000744.1, NCBI Ref. Seq.: NC_009656.1) swapping the α-helical structures from OprM for the homologous ones of OprA identified by sequence analysis and structure prediction showed in Figure 2. The chimera genes were synthesised by Thermo Fisher Scientific (Waltham, MA, USA) and subsequently amplified by PCR.

The pUC18T-miniTn7T-Lac-Gm backbone and *mexXY* gene were amplified from plasmid pPLS454 from using the primers listed in Table 3. Afterward, the *oprM/oprA* PCR

fragment was cloned into pUC18T-miniTn7T-Lac-Gm-*mexXY* using the Gibson Assembly Cloning Kit (New England Biolabs, Ipswich, MA, USA) as described in Appendix 1 into Invitrogen *E. coli* ElectroMAX™ DH5α-E Competent Cells (Thermo Fisher Scientific). Plasmid constructs were confirmed by PCR, restriction digest with EcoRI and SmaI enzymes (New England Biolabs, Ipswich, MA, USA) as well as Nanopore whole plasmid sequencing by Plasmidsaurus (Louisville, KY, USA).

All PCR products were obtained using VeriFi® polymerase by PCR Biosystems Ltd (London, UK), with thermal cycles described in Appendix 2 and appendix 3.

To understand the role of each swapped α-helical fragment in substrate selection, the efflux pump-deficient *P. aeruginosa* strain PAO750 was complemented with the *mexXY-oprM/oprA* chimera operon. Operon complementation using the miniTn7 construct was carried out using electroporation and subsequent Flp-mediated excision of the Gm marker cassette as described previously (Choi & Schweizer, 2006) resulting in seven *P. aeruginosa* strains with one OMP modification in each.

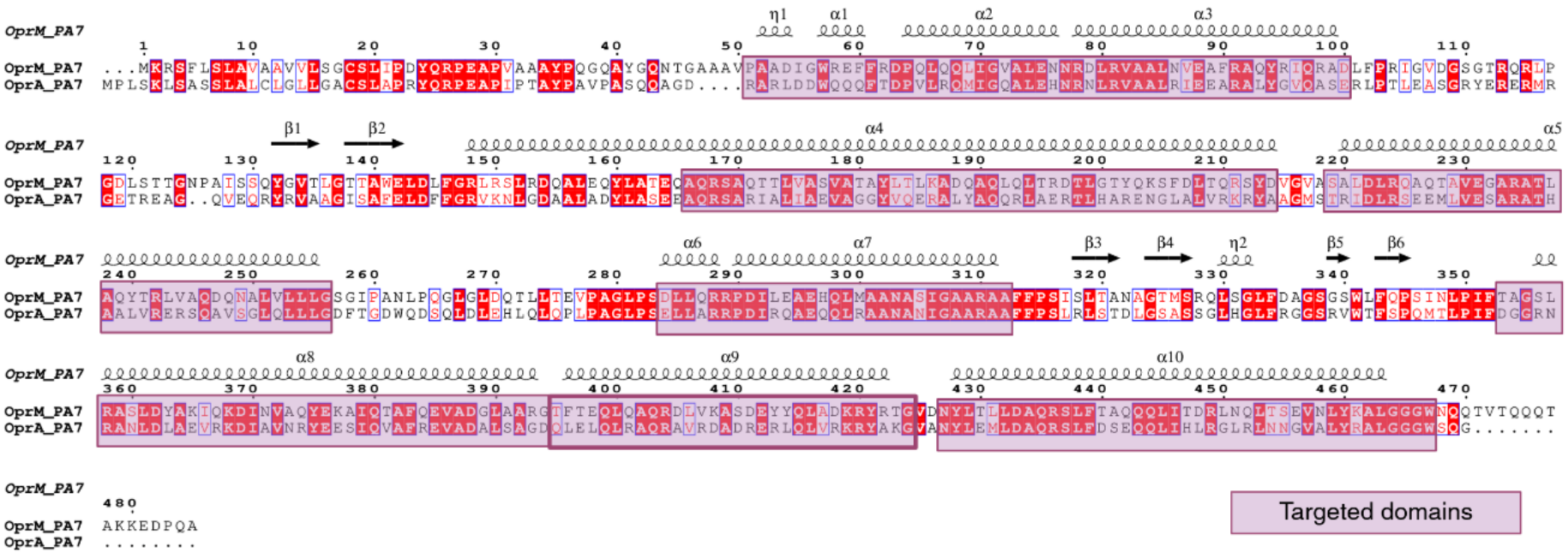

Figure 2 Alignment of OprM and OprA amino acid sequences from clinical isolate *P. aeruginosa* PA7. Sequences sourced from NCBI PA7 genome (Roy et al., 2010), OprM accession number ABR82805.1 and OprA accession number ABR81584.1. Alignment processed through Clustal Omega: Multiple Sequence Alignment tool from EMBL-EPI. Secondary structure element identification was completed with ESPript 3.2 using the Protein Data Bank (PBD) ID 1WP1(Akama et al., 2004). Highlighted sections correspond to α-helix domains swapped between OprM and OprA.

Table 1 List of strains used in this study

Strain	Genotype	Reference
DH5α	F– φ80*lac*ZΔM15 Δ(*lac*ZYA-*arg*F)U169 *rec*A1 *end*A1 *hsd*R17(r_K–, m_K+) *gal pho*A *sup*E44 λ-*thi*-1 *gyr*A96 *rel*A1	Invitrogen
PA7	Clinical isolate of *P. aeruginosa*	DSM 24068
PAO750	*ΔmexAB-oprM, ΔmexCD-oprJ, ΔmexEF-oprN, ΔmexXY*	(Kumar et al., 2006)
PAAK115	PAO750::*lacIq-mexXY*$_{PA7}$*-oprA*$_{PA7}$	(Singh et al., 2020)
PAAK238	PAO750::*lacIq-mexXY*$_{PA7}$*-oprM*$_{PA7}$	Kumar Lab Database
PAAK285	PAO750::*lacIq-mexXY*$_{PA7}$*-oprM*$_{PA7}$*/oprAα1_3*	This study
PAAK286	PAO750::*lacIq-mexXY*$_{PA7}$*-oprM*$_{PA7}$*/oprAα4*	This study
PAAK287	PAO750::*lacIq-mexXY*$_{PA7}$*-oprM*$_{PA7}$*/oprAα5*	This study
PAAK288	PAO750::*lacIq-mexXY*$_{PA7}$*-oprM*$_{PA7}$*/oprAα6_7*	This study
PAAK289	PAO750::*lacIq-mexXY*$_{PA7}$*-oprM*$_{PA7}$*/oprAα8_9*	This study
PAAK290	PAO750::*lacIq-mexXY*$_{PA7}$*-oprM*$_{PA7}$*/oprAα9*	This study
PAAK291	PAO750::*lacIq-mexXY*$_{PA7}$*-oprM*$_{PA7}$*/oprAα10*	This study

Table 2 List of plasmids used in this study

Plasmid	Features	Reference
pUC18T-miniTn7T-Lac-Gm	miniTn7-based single copy insertion plasmid, Amp^r, Gm^r.	(Choi et al., 2005)
pTNS2	Encodes to site-specific TnsABCD transposase for chromosome insertion, Amp^r.	(Choi et al., 2005)
pFLP2	Encodes FLP recombinase for Gm^r-cassette removal, Cb^r, *sacB*	(Hoang et al., 1998)
pPLS454	pUC18T-miniTn7T- *mexXY*$_{PA7}$-*oprM* $_{PA7}$	Kumar Lab collection
pPLS480	Synthetic gene fragment *oprM/oprAα1_3,* Amp^r	Purchased from GeneArt, ThermoFisher
pPLS481	Synthetic gene fragment *oprM/oprAα4,* Kan^r	Purchased from GeneArt, ThermoFisher
pPLS482	Synthetic gene fragment *oprM/oprAα5,* Kan^r	Purchased from GeneArt, ThermoFisher
pPLS483	Synthetic gene fragment *oprM/oprAα6_7,* Kan^r	Purchased from GeneArt, ThermoFisher
pPLS484	Synthetic gene fragment *oprM/oprAα8_9,* Kan^r	Purchased from GeneArt, ThermoFisher
pPLS485	Synthetic gene fragment *oprM/oprAα9,* Kan^r	Purchased from GeneArt, ThermoFisher
pPLS486	Synthetic gene fragment *oprM/oprAα10,* Kan^r	Purchased from GeneArt, ThermoFisher
pPLS487	pUC18T-miniTn7T-*mexXY*$_{PA7}$-*oprM/oprAα1_3*	This study
pPLS488	pUC18T-miniTn7T-*mexXY*$_{PA7}$-*oprM* $_{PA7}$*/oprAα4*	This study
pPLS489	pUC18T-miniTn7T-*mexXY*$_{PA7}$-*oprM* $_{PA7}$*/oprAα5*	This study
pPLS490	pUC18T-miniTn7T-*mexXY*$_{PA7}$-*oprM*$_{PA7}$*/oprAα6_7*	This study

pPLS491	pUC18T-miniTn7T-*mexXY*$_{PA7}$-*oprM*$_{PA7}$/*oprAα8_9*	This study
pPLS492	pUC18T-miniTn7T-*mexXY*$_{PA7}$-*oprM*$_{PA7}$/*oprAα9*	This study
pPLS493	pUC18T-miniTn7T-*mexXY*$_{PA7}$-*oprM*$_{PA7}$/*oprAα10*	This study

Table 3 List of oligonucleotides used in this study

ID no.	Primer	Sequence (5'→3')	Purpose	Reference
2553	MiniTn7-mexX-BB-R	GATGTGCATGGATGTCCCTCGGATTCCACTAGTGAGCTCGAA	Cloning	This study
2237	Mini-Tn7-Backbone-XY-PA7-F	GCAGGCCTGAGCAGGCCAACCAGATAAGTG	Cloning	This study
2554	G-mexXY-F	GAGCTCACTAGTGGAATCCGAGGGACATCCATGCACATC	Cloning	This study
2555	G-mexXY-R	GGACCTTTTCATCAGGTCAGCTCCGTTG	Cloning	This study
2556	G-oprM-PA7-F	GCTGACCTGATGAAAAGGTCCTTCCTTTCC	Cloning	This study
2240	oprM-PA7-R	GTTGGCCTGCTCAGGCCTGCGGATCTTCCT	Cloning	This study
72	PAglmsDn	GCACATCGGCGACGTGCTCTC	Chromosomal insertion	(Choi & Schweizer, 2006)
73	Tn7R	CACAGCATAACTGGACTGATTTC	Chromosomal insertion	(Choi & Schweizer, 2006)

2.1.3 Antibiotic susceptibility assay

The Minimum inhibitory concentration (MIC) assay was conducted following the Clinical Laboratory Standards Institute guidelines (CLSI, 2018). In summary, overnight cultures in LB media were prepared from isolated colonies of each bacterial strain of interest and sub-cultured in a 1:100 (v/v) dilution in fresh LB and grown until an OD_{600} = 0.3-0.4 (3 hours for consistency); for strains that required induction, IPTG was added to a final concentration of 1 mM and incubated for 3 more hours. In 96-well round bottom plates, antibiotics were serially diluted by two-fold in sterile cation-adjusted Muller Hinton Broth (CA-MHB) (Oxoid) with 20 mg/L Ca^{2+} (as $CaCl_2 \cdot 2H2O$) and 12.5 mg/L Mg^{2+} (as $MgCl_2 \cdot 6H2O$) (Barry et al., 1992). Medium without additives, antibiotic and positive controls were included in each experiment.

The sub-cultured bacteria were standardized to 0.50 ± 0.02 McFarland (equivalent to 1.5 x 10^8 CFU/mL) in 2 ml of sterile 0.85% NaCl using a DensiCHECK Plus Instrument (BioMerieux). Standardized cells were added in a 1:50 (v/v) dilution in CA-MHB and used to inoculate the two-fold antibiotic plates. IPTG was also added to the bacterial CA-MHB dilutions to facilitate continuous induction and expression. The plates were statically incubated for 18 ± 2 hours at 37°C.

2.1.4 Ethidium bromide agar susceptibility assay

To assess efflux pump functionality, 10-fold dilutions of each strain were spot-plated onto medium supplemented with ethidium bromide (EtBr). Increased survival upon induction was used as an indicator of MexXY-OprM/OprA complex activity.

Overnight cultures were grown in LB broth and sub-cultured in a 1:100 (v/v) dilution in fresh LB broth for 3 hours. One millimolar IPTG was added to strains that required induction, and cultures were incubated for 3 additional hours. Cells were standardized to 0.5 ± 0.02 McFarland and serially diluted 1:10, 8 times in sterile saline solution (0.85% NaCl). Three microliters of each dilution were spotted on cation adjusted-Muller Hinton agar (CA-MHA) plates containing 2 µg/mL ethidium bromide and CA-MHA + 2 µg/mL ethidium bromide + 1 mM IPTG; CA-MHA + 1 mM IPTG and CA-MHA were included for growth controls. Plates were incubated at 37°C for 18-20 hours and images were captured on a Gel Doc Imaging System (Axygen, Oakville, Canada) with white light and an exposure time of 51 msec.

2.1.5 Mutant OMP structure prediction

Mutant OprM/OprA outer membrane factors designed as described in Section 2.1.2 were used to generate the protein structure. Each one-letter amino acid sequence was submitted in ColabFold v1.5.5, a collaboratory implementation of the AlphaFold2 algorithm (Mirdita et al., 2022), using default parameters. The resulting models were generated for both the monomeric and trimeric forms of each of the mutants. For improved accuracy, only models with an average pLDDT (predicted Local Distance Difference Test) score above 90 were selected

2.2 Results

2.2.1 *mexXY-oprM/oprA* chimera operon construction into miniTn7 system and strain complementation

As mentioned before, seven constructs, listed in Table 2, were created by replacing the α-helix domains from OprM, highlighted in Figure 2, by the corresponding region from OprA, as indicated on Table 4 and cloned into *E. coli* DH5α in a pUC18T-miniTn7T-Lac-Gm backbone. These chimeric constructs were expressed as single gene copies of the mutant operon under the control of the IPTG inducible P_{tac} promoter, allowing controlled assessment of their functional impact.

Prior to the insertion in the *P. aeruginosa* host strain, the correct construct assembly was confirmed by restriction digest and nanopore plasmid sequencing.

The miniTn7 system was selected for strain complementation due to its efficient use. The TnsABCD transposase components of Tn7 promote high-frequency, site- and orientation-specific insertion into the *P. aeruginosa* bacterial chromosome at Tn7 attachment (*att*Tn7) sites located downstream of the extremely conserved *glmS* gene encoding glucosamine-6-phosphate synthetase (Choi & Schweizer, 2006; Craig, 1991).

To confirm insertion of each construct into the efflux pump-deficient *P. aeruginosa* PAO750 strain, PCR was performed using the primers PAglmsDn and Tn7R (Table 3), resulting in a single DNA fragment of 272 bp (Figure 3A). Also, as a precaution, the presence of the genes of interest *mexXY* (4387 bp) and *oprM/oprA* (1477 bp) were confirmed in each strain (Figure 3B and Figure 3C, respectively) using primers listed in Table 3. This confirmed the genotypes of the seven resulting strains used in this study

complemented with the *mexXY-oprM/oprA* chimeric operon with one single α-helix mutation each.

PAO750 strains expressing *mexXY*$_{PA7}$-*oprM*$_{PA7}$ operon (PAAK238) and *mexXY*$_{PA7}$-*oprA* operon (PAAK115) were created previously in the Kumar Lab by Dr. Yanqi (Colin) Li and Dr. Manu Singh, respectively, and were employed as reference strains.

Table 4 Swapped domains.

Target domain	**OprM → OprA**
α1_3	P^{51}-D^{100} → R^{50}-E^{99}
α4	A^{166}-D^{214} → A^{163}-A^{211}
α5	S^{219}-G^{256} → T^{216}-G^{253}
α6_7	D^{284}-A^{312} → E^{281}-A^{309}
α8_9	T^{353}-T^{423} → D^{350}-K^{420}
α9	T^{395}-T^{423}→ D^{350}-K^{420}
α10	N^{427}-G^{466}→ N^{424}-G^{463}

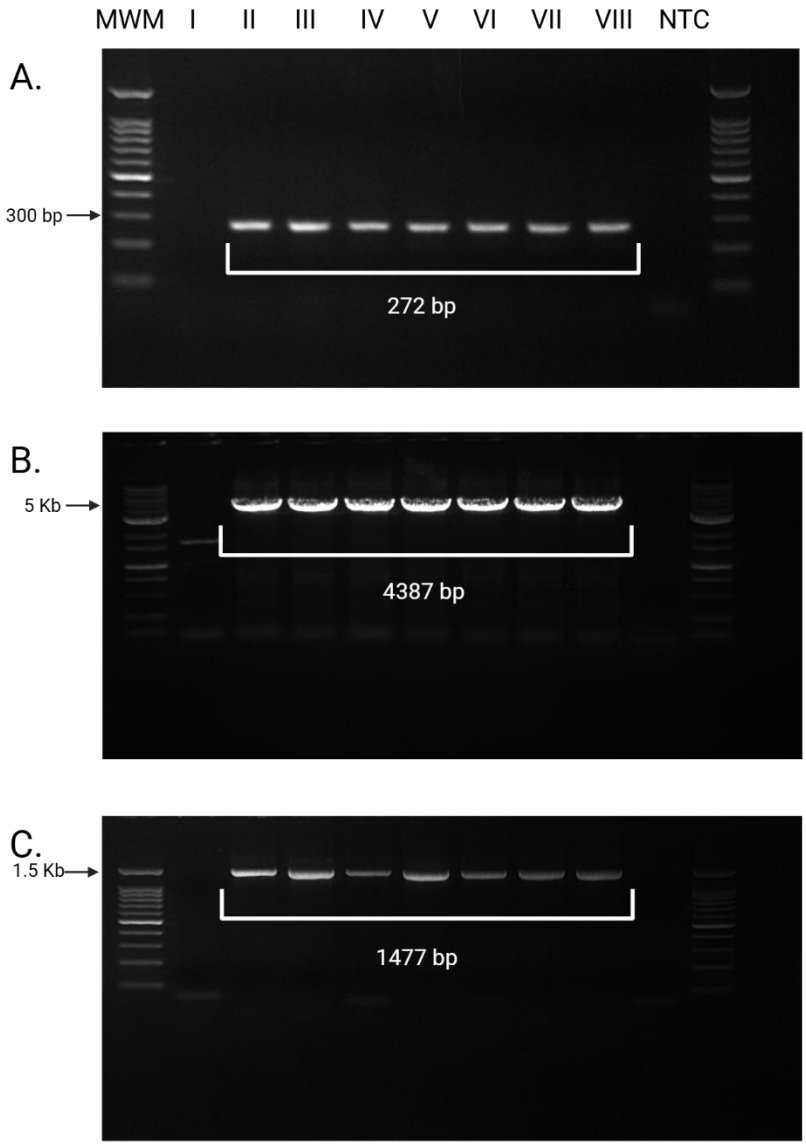

Figure 3 Confirmation of mutant *mexXY-oprM/oprA* operon insertion in *P. aeruginosa* PAO750 by PCR. Agarose gel electrophoresis of PCR products from screening of (A) chromosomal insertion at *att*Tn7 site, (B) *mexXY* presence and (C) *OprM/OprA* precense. MWM lane corresponding to molecular weight marker (A and C) used was 100 bp DNA ladder (FroggaBio) and (B) 1 KB plus DNA ladder (FroggaBio). Strain denotation (from left to right): **I.** PAO750, **II.** PAAK285 (PAO750::*mexXY*$_{PA7}$*-oprM/oprAα1_3*), **III.** PAAK286 (PAO750::*mexXY*$_{PA7}$*-oprM/oprAα4*), **IV.** PAAK287(PAO750::*mexXY*$_{PA7}$*-oprM/oprAα5*), **V.** PAAK288 (PAO750::*mexXY*$_{PA7}$*-oprM/oprAα6_7*), **VI.** PAAK289(PAO750::*mexXY*$_{PA7}$*-oprM/oprAα8_9*), **VII.** PAAK290 (PAO750::*mexXY*$_{PA7}$*-oprM/oprAα9*), **VIII.** PAAK291(PAO750::*mexXY*$_{PA7}$*-oprM/oprAα10*).

2.2.2 Chimera OMP OprM/OprA form a functional complex with MexXY in *P. aeruginosa* complements

The EtBr susceptibility assay was performed to evaluate the functionality of the pumps. Where increased survival after the induction of expression of the efflux pump was used as indicator the complex activity as EtBr accumulation is toxic to the cells and with higher survival, efflux of this molecule can be inferred.

In the controls, induction of the MexXY-OprM efflux pump (strain PAAK238) increased EtBr tolerance by 10-fold, as induced cells remained viable up to the 10^{-4} dilution whereas non-induced cells grew only to 10^{-3}. In the case of the MexXY-OprA induced efflux pump (PAAK115 strain), the EtBr tolerance increased by 100-fold as induced cells grew up to the 10^{-6} dilution in comparison to non-induced cells growing only to 10^{-4} dilution.

Among the chimeric constructs, two strains exhibited notably higher EtBr resistance compared to the others; strain PAAK286, expressing the *mexXY-oprM/oprAα4* chimera, displayed a 100-fold increase in survival, while PAAK288 (*mexXY-oprM/oprAα6_7*) showed a 1000-fold (Figure 4) increase. Both mutant strains remained viable up to the 10^{-8} dilution upon induction. In contrast, the remaining OMP mutant strains showed only a 10-fold increase in EtBr resistance, with growth up to the 10^{-5} dilution under induction compared to the 10^{-4} dilution in the absence of IPTG.

PAO750 strain, which does not express any efflux pump, displayed the same survival range in the presence of EtBr regardless of IPTG addition, confirming that IPTG presence alone does not influence EtBr tolerance in the absence of an efflux system.

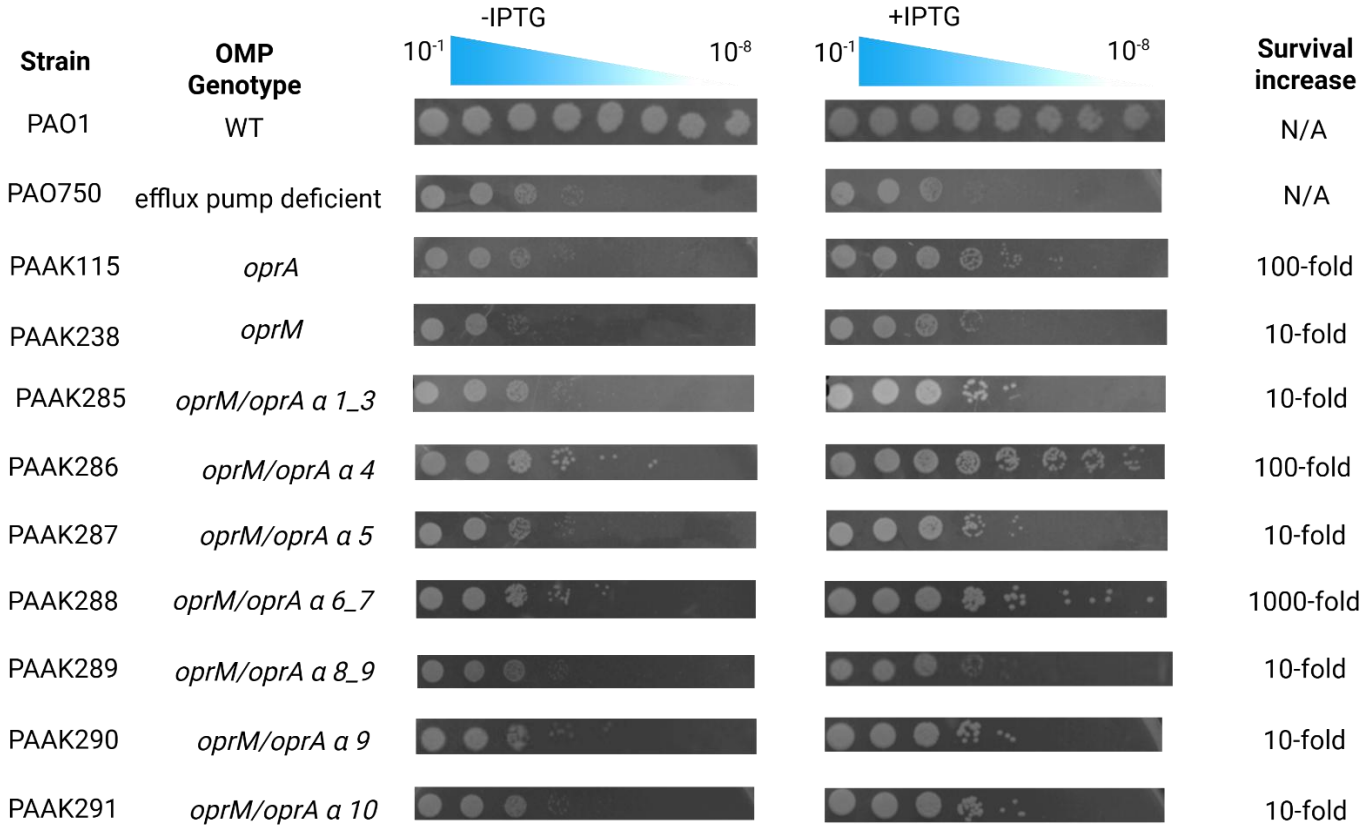

Figure 4 Ethidium bromide susceptibility of efflux mutant strains. Strains were plated onto 2 µg/mL ethidium bromide. Highest cell concentration on the left as indicated by the gradient (10-fold dilution starting with 10^{-1} in both conditions). Each assay was performed with three biological replicates and three technical replicates. Strains in the right column were induced with 1mM IPTG and those in the left column are non-induced. Strain genotype is listed in Table 1. Image color correction was done with brightness +20% and contrast -40%. Representative of three biological replicates and three technical replicates each.

2.2.3 Antibiotic substrate selection in *P. aeruginosa* MexXY-OprM/OprA mutant strains

Minimum inhibitory concentration (MIC) assays were performed to assess the substrate specificity (Table 5) of the *P. aeruginosa* OMP mutant panel. Gentamicin (Gm) and tetracycline (Tet) were included as control substrates, as both are well-established substrates of the OprM and OprA OMP efflux channels. To evaluate the contribution of the α-helix region to substrate selection, mutant strains were additionally tested against carbenicillin (Cb) and sulbenicillin (Sb), two β-lactams previously shown to be expelled by MexXY-OprA but not by MexXY-OprM. This experimental design allowed the examination of how α-helix modifications influence differential antibiotic recognition and efflux capacity.

Most of the mutant strains exhibited no detectable change in Gm MIC upon induction. Only three strains showed increased gentamicin resistance: PAAK290 displayed a 2-fold increase (similar to the PAAK115 control), PAAK285 (PAO750:: *mexXY-oprM/oprA α1_3*) showed a 4-fold change (comparable to PAAK238 control) and PAAK288 exhibited the largest response with an 8-fold increase in MIC.

In contrast to the gentamicin results, all of the mutant strains exhibited at least a 2-fold increase in tetracycline resistance upon induction. The most pronounced increases were observed in PAAK288, which showed a 64-fold increase in MIC, followed by PAAK285 with 32-fold increase (which is similar to the PAAK238 control). PAAK290 and PAAK291 both displayed an 8-fold increase in tetracycline MIC.

The results of the β-lactams carbenicillin (Cb) and sulbenicillin (Sb) are as follows. For Cb, four of the seven mutants exhibited a 2-fold change in MIC — PAAK287(PAO750::*mexXY-oprM/oprA α5*), PAAK288, PAAK289 (PAO750::*mexXY-oprM/oprA α8_9*) and PAAK290 (PAO750::*mexXY-oprM/oprA α9*) — which is comparable to the PAAK238 control but substantially lower than the 16-fold increase observed in the PAAK115 control. The remining strains showed no change in their values after induction.

Contrary to Cb results, PAAK285 and PAAK291 showed a 2-fold increase to Sb resistance, similar to MexXY-OprM control, whereas PAAK290 again demonstrated a modest 2-fold increase consistent with its Cb profile. PAAK286 showed a 4-fold increase and the MexXY-OprA control exhibited the strongest response, as expected, with an 8-fold increase resistance to Sb. The rest of the mutant strains did not exhibit any Sb MIC change upon IPTG induction.

In summary, it was observed a gain of activity from the PAAK286 mutant strain to expel sulbenicillin, while PAAK 288 and PAAK290 showed recovery of activity expelling tetracycline and gentamicin to the same MIC as PAAK215 control strain expressing MexXY-OprA. These observations are consistent with the EtBr susceptibility results where the PAAK286 and PAAK288 strains showed the highest EtBr resistance when the efflux pump expression was induced with IPTG.

Table 5 Antibiotic susceptibility profile of mutant OMP strains. Antibiotic susceptibility was performed with the two-fold broth microdilution method in CA-MHB. MIC value presented in µg/ml. Where values highlighted in yellow represent the OprA complex reference MIC and the gradient of orange represent MIC values higher than OprA, equal to OprA or lower than OprA but higher than OprM. Representative of three biological replicates and three technical replicates each.

		Gm		Tet		Cb		Sb	
Strain	Genotype	-	+	-	+	-	+	-	+
PA0750	non-efflux pumps	0.5	0.5	0.25	0.25	0.5	0.5	2	2
PAAK115	*mexXY-oprA*	2	4	4	64	0.5	8	2	16
PAAK238	*mexXY-oprM*	0.5	2	0.25	8	0.5	1	2	4
PAAK285	*mexXY-oprM/oprA α1_3*	0.5	2	0.5	16	1	1	2	4
PAAK286	*mexXY-oprM/oprA α4*	1	1	8	32	1	1	4	16
PAAK287	*mexXY-oprM/oprA α5*	0.5	0.5	0.25	0.5	0.5	1	2	2
PAAK288	*mexXY-oprM/oprA α6_7*	1	8	1	64	0.5	1	4	4
PAAK289	*mexXY-oprM/oprA α8_9*	0.5	0.5	0.25	0.5	1	2	4	4
PAAK290	*mexXY-oprM/oprA α9*	2	4	4	32	1	2	2	4
PAAK291	*mexXY-oprM/oprA α10*	0.5	0.5	0.25	2	0.5	0.5	2	4

Gm, gentamicin; Tet, tetracycline; Cb, carbenicillin; Sb, sulbenicillin. “-”, no IPTG added; “+”, 1 mM IPTG added.

2.2.4 Chimera OprM/OprA structure analysis

Each chimeric OMP was analysed and compared with the OprM crystal structure published by Akama *et al.* (2004; PDB ID: 1WP1). Structural comparisons were focused on the equatorial region and the periplasmic end of the trimer, as all engineered modifications were confined to α-helix segments within the equatorial and coiled-coil domains.

For equatorial measurements, the diameter was calculated as the distance between residues on opposing protomers. In the chimeric constructs, the distance between Phe^{383} and Val^{175} was used, except for OprM/OprAα4 chimera, in which the corresponding residue was Ile^{175} due to the helix substitution. For the OprM reference structure, the equivalent residues were Leu^{157} and Glu^{368}. These positions were selected because they are located at the widest portion of the channel.

To measure the diameter of the periplasmic end, the distance between the Leu^{429} of each protomer was obtain for all the chimeras, and the homologous residue Leu^{412} was used for the OprM reference. These residues were selected due to their proximity in the periplasmic end. The measurements were taken in the three chains of the complex and then averaged to obtain the final values.

Manual measurements in the present analysis yielded diameters of ~31 Å at the equator and 4 Å at the periplasmic end for the reference structure. Using these values as baselines, the chimera proteins were evaluated. All engineered structures displayed an enlarged equatorial diameter between 43-45 Å corresponding to approximately a 28% increase relative to the OprM reference.

In contrast, the periplasmatic-end diameter displayed minimal deviation from the reference in most constructs, with values ranging from 4.2-4.4 Å. Three chimeras differed substantially: OprM/OprAα5 exhibited a reduced diameter of ~3.81 Å which is approximately 13% smaller than the OprM reference; OprM/OprAα8_9 showed a diameter of 7.9 Å and OprM/OprAα9 displayed a diameter of 8.2 Å, representing 79% and 86% increase versus the reference, respectively.

The analysis of the extracellular end of the predicted proteins (Figure 5.II) showed that the diameters of the exit side have a size reduction between 7% and 15%, with the smallest diameter corresponding to the OprM/OprAα10 mutant with 7.5 Å and the largest to the mutants OprM/OprAα6_7 and OprM/OprAα8_9 with a diameter of 8.2 Å.

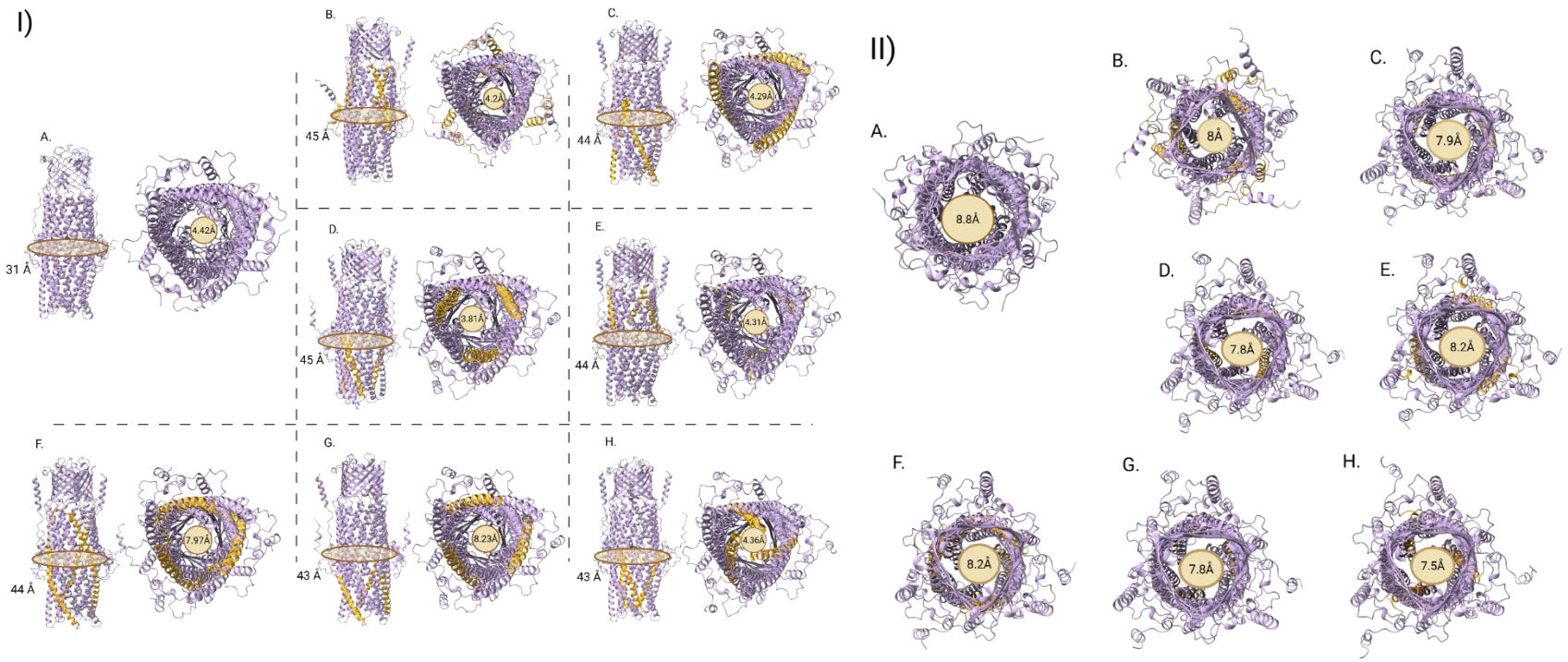

Figure 5 Predicted structures of outer membrane channel chimeras. OMP models were generated using ColabFold v1.5.5 and visualized in ChimeraX 1.9. Regions derived from OprA are highlighted in orange, while conserved OprM segments are shown in purple. For each construct, in section I), the left panel displays the trimeric OMP in a side (vertical) view with equatorial approximate pore diameter measurement, and the right panel shows a cross-sectional (horizontal) periplasmic-end (entrance) view with the approximate pore aperture diameter indicated. Shown in section II) is the extracellular side of the protein (exit side) with the approximate pore aperture diameter indicated. (A) OprM (PDB: 1WP1). (B) OprM/OprAα1–3. (C) OprM/OprAα4. (D) OprM/OprAα5. (E) OprM/OprAα6–7. (F) OprM/OprAα8–9. (G) OprM/OprAα9. (H) OprM/OprAα10

2.3 Discussion

This study was focused on understanding the role of the α-helix domains of the OMPs —OprM and OprA — in the substrate selection within the MexXY RND efflux system in *P. aeruginosa.* To address this, the efflux pump-deficient strain PAO750 was complemented with the MexXY and a series of chimeric OprM/OprA outer membrane channels.

Comparative analysis of chimeric OprM/OprA constructs was performed using *in silico* structural modeling, functional efflux assays, and antibiotic susceptibility profiling to evaluate how α-helical substitutions influence OMP behavior within the assembled RND efflux complex.

EtBr susceptibility agar assays were used as an initial functional readout to assess the ability of the mutant complexes to expel a common efflux substrate. Survival in EtBr-containing medium is indicative of active efflux, as intracellular accumulation of EtBr is toxic (X. Z. Li et al., 2003).The efflux pump-deficient strain PAO750 exhibited growth in the EtBr-supplemented media only up to the 10^{-3} dilution, whereas all strains expressing chimeric OMPs showed at least a 10-fold survival increase. This indicates that the observed survival is attributable to restored efflux activity rather than other resistance mechanisms (Kyriacou et al., 2002) and that α-helical substitutions did not abolish efflux pump assembly or transport activity.

A notable EtBr resistance increase was observed in the strains PAAK286 (helix α4 mutant) and PAAK288 (helix α6_7 mutant) even in the absence of IPTG. Although IPTG is an effective inducer, the *LacI-Ptac* system is known to exhibit intrinsic leakiness where

the expression of target genes can be observed in absence of an inducer (Asensio-Calavia et al., 2024). However, upon induction these strains exhibited the highest survival rate increases with 100-fold and 1000-fold higher resistance, respectively. This suggests that specific α-helical substitutions may enhance efflux efficiency without compromising complex assembly.

Previous studies by Singh *et al*. (2020) showed that the MexXY-OprA complex from *P. aeruginosa* (renamed as *P. paraeruginosa*) PA7 strain is able to efflux the β-lactams carbenicillin and sulbenicillin in addition to aminoglycosides. This substrate profile differs from the observed when MexXY from PA7 forms a complex with OprM from PAO1. In contrast the study presented in this thesis, showed that when MexXY formed a complex with OprM, both from PA7, the efflux from carbenicillin and sulbenicillin had a two-fold increase compared to the MexXY-OprA complex with 16-fold and 8-fold change resistance increase to carbenicillin and sulbenicillin, respectively.

It is thought that the α-barrel structure of the OMP interacts directly with the α-hairpin domain of the PAP forming an extended helical bundle that connects the inner membrane structure to the outer membrane channel (Symmons et al., 2009). For this reason, this study focused on examining if α-helical domains are involved in the substrate selection of the RND-complex and evaluating the interaction of OMP with the PAP.

We observed that when the α4 domain of OprM was swapped with the corresponding domain from OprA (strain PAAKA286), the sulbenicillin MIC was restored to the level observed of the MexXY-OprA complex but the carbenicillin MIC was not. This domain is located within the H3 coiled-coils, which in similar proteins such as the CmeC channel from *Campylobacter jejuni,* are in direct contact with the PAP. This interaction

has been proposed to regulate the opening and closing mechanism of the OMP during drug extrusion (Lei Dai, 2016).

Although only one mutant strain gained activity against sulbenicillin to the level of MexXY-OprA, other mutants showed restored the MIC values for different antibiotics. In summary, PAAK288 (helix α6_7 mutant) restored resistance to tetracycline and gentamicin, while PAAK290 (helix α9 mutant) restored gentamicin resistance comparable to the MexXY-OprA complex. The remaining strains maintained activity similar to the MexXY-OprM complex for the antibiotics tested.

Interesting intermediate phenotypes were observed where levels of resistance did not reach those of the MexXY-OprA complex but showed higher activity than the MexXY-OprM. Some examples include PAAK286 with tetracycline efflux, PAAK288 with gentamicin efflux, PAAK289 (helix α8_9 mutant) with carbenicillin efflux and PAAK290 with tetracycline and carbenicillin efflux.

These observations suggest that the introduced mutations in this study may alter the interaction within the MexXY-OprM complex (Yoshihara et al., 2009), enhancing efflux efficiency of different antibiotics.

Structural analysis was performed using predicted models of the chimeric proteins. However, confirmation of these observations, would require experimental determination using techniques such as X-ray crystallography. Previous structural studies of OprM from PAO1 reported an equatorial diameter of ~25 Å, a fully occluded periplasmic end and an extracellular side not larger than 3 Å in a closed state (Akama et al., 2004; Phan et al., 2010). The manual measurements realized in this study differed from these reported

values with some mutants periplasmatic end diameter of up to 8.23Å and 8Å extracellular end of the protein; however, openings in the periplasmic side must be of at least 10 Å to allow big molecules such as antibiotics to pass through (Phan et al., 2010) discarding the possibility non-selective efflux of antibiotics.

Several studies support a dynamic gating mechanism where the flexibility of the coiled-coil domain and the equatorial domain of the OMP play an important role in the efflux of molecules due to its interaction with the PAP (Phan et al., 2015; Yamanaka et al., 2007). However, these studies reveal only efflux activity and there are no previous studies that may indicate substrate selection. As mentioned before, the only mutant strain that showed gain of function was PAAK286 and the mutation is located in the equatorial and coiled-coil domain of the protein.

These findings may indicate that substitutions within specific α-helical segments located in the coiled-coil and the equatorial domain can significantly alter the substrate selectivity of the efflux pump due to changes in the interaction with the PAP.

2.4 Conclusion and future directions

While the findings in this study provide an insight to the role of α-helical domains in the OMP for the substrate selection of the complex, the mechanism of substrate selection and substrate binding site remains unclear. To fully elucidate this knowledge gap, additional work is required.

According to findings described in this study, the next steps should be focusing in the α4-domain, swapping smaller sections of the domain and possibly creating single nucleotide mutations to determine if those changes have an effect in the substrate selectivity of the pump, as well as test broader range of substrates. Also, as mentioned before, the validation of the structure is recommended by technics such as X-ray crystallography or Cryo-Electron Microscopy (cryo-EM) in the presence of a substrate and without substrate to have a better understanding of the structure modifications involved in the efflux of molecules.

Chapter III: *mexXY-oprA* operon prevalence in *Pseudomonas* spp.

3.1 Materials and methods

3.1.1 Identification of *mexXY-oprA* operon in *Pseudomonas* spp.

The *mexXY-oprA* operon sequence from *Pseudomonas paraeruginosa* PA7 (NCBI RefSeq accession NC_009656.1) was used as the query for nucleotide sequence comparison within *Pseudomonas* spp. using BLASTn (version 2.17.0+) (Zhang et al., 2000). Searches were performed against the RefSeq Genome database (refseq_genomes), restricting the organism selection to "*Pseudomonas* Migula 1894" (Approved list 1980; taxid: 286), "*Pseudomonas aeruginosa*" (taxid: 287) and "*Pseudomonas paraeruginosa*" (taxid: 2994495). The maximum number of target sequences was set to 500, while all other parameters were kept at default settings.

Query coverage was used to assess the presence of the complete *mexXY–oprA* operon. Only whole genome sequence hits covering ≥90% of the full operon sequence with high sequence identity (≥90%) were considered indicative of an intact operon.

3.1.2. Comparative genomic organization of the *mexXY-oprA* operon

To assess conservation of the genomic context surrounding the *mexXY-oprA* operon, the BLAST query hits that met the criteria mentioned in section 3.1.1 were selected to perform comparative gene cluster analysis. Manually, protein-coding genes upstream and downstream of the operon were identified and extracted from each genome and input for CAGECAT clinker (van den Belt et al., 2023). Clinker was employed to generate comparative gene cluster visualization, enabling assessment of operon-associated gene conservation across *Pseudomonas* spp.

3.1.3. Phylogenetic analysis

To identify the species of the analysed sequences, a phylogenetic analysis was carried out. The *rpoB* gene from the organisms selected in the BLASTn analysis was used. The tree was rooted to the outgroup *Acinetobacter baumannii* ATCC 17978-VU (NZ_CP018664.1), the PA7 strain was used to identify the *P. paraeruginosa* and the PAO1 strain (NZ_CP199157.1) was used to identify *P. aeruginosa*.

The Maximum Likelihood (ML) method was used to infer the phylogeny with 1,000 replicates bootstrap consensus conducted in MEGA12 (Kumar et al., 2024)

3.2. Results

3.2.1. Identification and comparative synteny of the *mexXY-oprA* operon and surrounding genomic regions in *Pseudomonas* spp.

Sixteen whole-genome sequences were identified to contain the complete *mexXY-oprA* operon (Table 6), exhibiting >90% nucleotide identity and 100% query coverage relative to the PA7 reference sequence. BLAST hits displaying <100% query coverage corresponded to partial operon matches, in which *mexX* and *mexY* were detected in the absence of the *oprA* component.

Taxonomic classification using the NCBI database annotations indicated that five of the identified genomes belonged to *Pseudomonas paraeruginosa,* while the remaining eleven were classified as *Pseudomonas aeruginosa*. The *P. paraeruginosa* strains exhibited high conservation of the operon, with an average nucleotide identity of 99.65% relative to the PA7 reference strain sequence. In contrast, *P. aeruginosa* strains displayed lower identity overall (94%), except for strain A39-1, which showed 99.70% identity.

The identified strains originated from a diverse range of sources and geographical locations worldwide. These comprised environmental isolates recovered from soil, rivers and plant rhizosphere samples, as well as human clinical isolates associated from CF patients, and lung and urinary tract infections. In addition, veterinary clinical isolates recovered from cases of canine otitis were included

Table 6 Distribution and characteristics of *Pseudomonas* strains harboring the complete *mexXY-oprA* operon. Whole-genome sequences containing complete *mexXY-oprA* operon following BLASTn screening against the RefSeq Genome Database. Inclusion criteria required ≥90% nucleotide identity and 100% query coverage relative to the *Pseudomonas paraeruginosa* PA7 reference operon (NC_009656.1). Species designation and sample source metadata were obtained from NCBI RefSeq records.

Species	Strain	NCBI ref.	Nucleotide identity (%)	Isolation Source / Host
Pseudomonas paraeruginosa	PA7	NC_009656.1	100%	Host: *Homo Sapiens* Non-respiratory isolate. Argentina
Pseudomonas paraeruginosa	AZPAE15042	NZ_CP041354.1	99.70%	Host: *Canis Lupus familiaris*. Host disease: Otitis externa. Isolation: Ear canal swab. UK
Pseudomonas paraeruginosa	Zw26	NZ_CP109657.1	99.70%	Host: *Homo Sapiens* Host disease: Cystic Fibrosis. Germany
Pseudomonas aeruginosa	A39-1	NZ_CP068238.1	99.70%	Soil. China
Pseudomonas paraeruginosa	AR441	NZ_CP029093.1	99.69%	-
Pseudomonas paraeruginosa	AR_0356	NZ_CP027169.1	99.69%	-
Pseudomonas paraeruginosa	Cr1	NZ_CP020560.1	99.65%	*Chilli rhizosphere*. India
Pseudomonas aeruginosa	Paer74	NZ_CP114093.1	94.25%	Host: *Homo sapiens* Host disease: lung infection. Isolation: Sputum. Belgium
Pseudomonas aeruginosa	PALA52	NZ_CP110347.1	94.25%	Host: *Homo Sapiens* Host disease: Cystic Fibrosis Isolation: Sputum. UK, London
Pseudomonas aeruginosa	H09	NZ_CP093021.1	94.23%	River. Germany

Pseudomonas aeruginosa	490614	NZ_CP173121.1	94.23%	Host: *Canis Lupus familiaris* Host disease: Otitis externa Isolation: Ear canal swab. UK
Pseudomonas aeruginosa	Paer84	NZ_CP114098.1	94.23%	Host: *Homo sapiens* Host disease: Lung infection Isolation: sputum. Belgium
Pseudomonas aeruginosa	SH3A	NZ_CP146217.1	94.23%	Host: *Homo Sapiens* Host disease: Cystic Fibrosis Isolation: Cell culture. UK, London
Pseudomonas aeruginosa	489267	NZ_CP173124.1	94.16%	Host: *Canis Lupus familiaris.* Host disease: Otitis externa. Isolation: Ear canal swab. UK
Pseudomonas aeruginosa	CMC-115	NZ_CP046602.1	94.16%	Host: *Homo Sapiens* Isolation: Tracheal aspirate. Host disease: HCAP- acute pneumonia. USA
Pseudomonas aeruginosa	484919	NZ_CP173128.1	94.14%	Host: *Canis Lupus familiaris.* Host disease: Otitis externa. Isolation: Ear canal swab. United Arab Emirates
Pseudomonas aeruginosa	488958	NZ_CP173125.1	94.12%	Urinary tract infection. Germany

The genomic context surrounding the mexXY-oprA operon was highly conserved, with fourteen upstream and fifteen downstream protein-coding genes consistently present across the analyzed strains (Figure 6). Overall, it was observed that the *mexXY-oprA* operon is highly conserved across the analyzed strains. The primary differences were observed in upstream regions, notably in the *mexZ* regulatory gene, showing sequence identity as low as 30% when compared to the *P. paraeruginosa* PA7 reference strain. Additionally, variability was observed in the presence of two hypothetical protein-coding genes located eleven and twelve genes upstream the operon, respectively, in six out of sixteen analyzed strains. Notably, no genes annotated as transposase, integrases or mobile genetic element-associated functions were detected within the genomic regions.

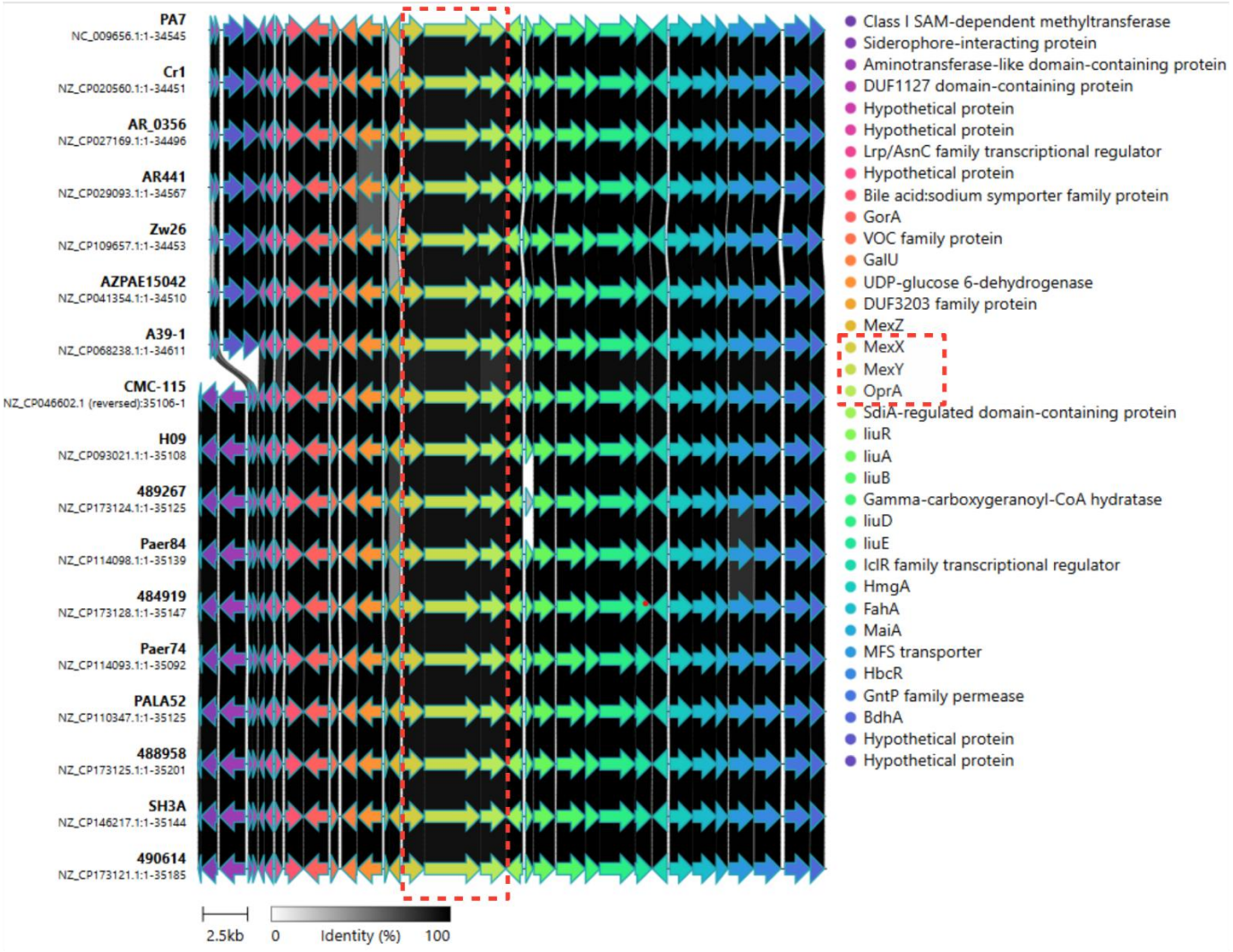

Figure 6 Comparative synteny of *mexXY-oprA* operon across *Pseudomonas* species. Aligned relative to the characterized genome from *Pseudomonas paraeruginosa* PA7 (NC_009656.1). Colored arrows represent annotated coding sequences with predicted functions. Shaded areas indicate regions of shared sequence identity, with darker shades corresponding to higher similarity. Synteny is shown only where supported by conserved gene order and sequence similarity. *mexX, mexY* and *oprA* genes can be identified inside the pointed square, with fourteen genes upstream and fifteen genes downstream of the operon. The figure was generated using CAGECAT Clinker.

3.2.2. Phylogenetic validation of species assignment

Phylogenetic reconstruction based on *rpoB* sequences (Figure 7) revealed two clear clades corresponding to *P. paraeruginosa* and *P. aeruginosa.*

According to NCBI database annotations, only five of the analyzed strains were classified as *P. paraeruginosa*. However, the *rpoB* phylogeny showed that fourteen of the sixteen strains (excluding PA7) clustered within the *P. paraeruginosa* clade, while only two strains grouped with *P. aeruginosa.* This discrepancy indicates that several strains may be misannotated in the NCBI database. Both *P. aeruginosa* strains containing the *mexXY-oprA* operon were isolated from patients with pneumonia and lung infections.

Furthermore, the distribution of *mexXY-oprA* across multiple sub-lineages within *P. paraeruginosa* indicates that the presence of this operon is not restricted to a single clonal lineage.

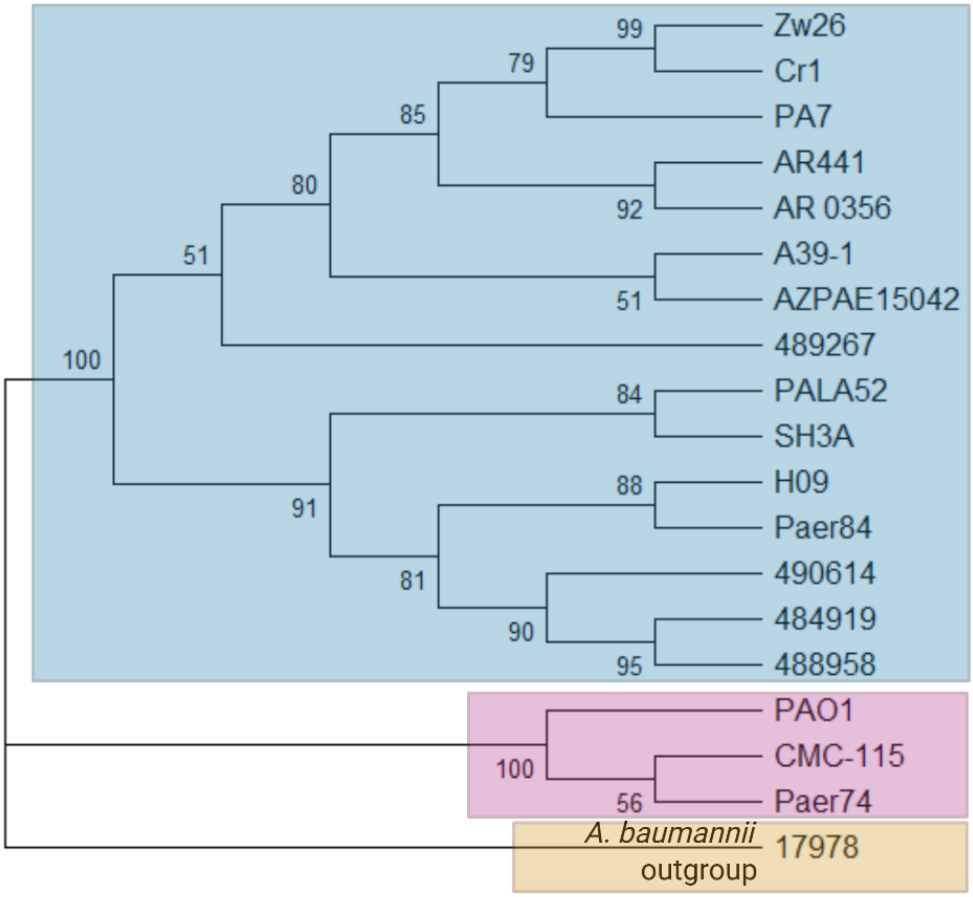

Figure 7 *rpoB*-based phylogenetic tree used for species-level classification of analyzed strains. Phylogenetic reconstruction based on *rpoB* nucleotide sequences performed to confirm species assignment of strains included in the *mexXY-oprA* operon analysis. Strains clustered in the blue box belong to *Pseudomonas paraeruginosa* species, while those within the pink box correspond to *P. aeruginosa*. *Acinetobacter baumannii* ATCC 17978-VU was included as an outgroup to root the tree and is highlighted in the yellow box. Bootstrap support values (%) are indicated at branch nodes.

3.3. Discussion

The *mexXY-oprA* operon had been reported in a small group of *P. aeruginosa* strains, particularly those belonging to the O12 serotype, such as the PA7 strain, and it has been suggested that some other strains had possessed the *oprA* gene but lost it (Morita et al., 2012b, 2012a). The PA7 strain was considered part of an outlier clade of *P. aeruginosa*; however, in 2022, it was proposed to be reclassified as its own novel species and was named *Pseudomonas paraeruginosa* (Rudra et al., 2022).

In order to determine the prevalence of the operon in *Pseudomonas* species, a search of the *mexXY-oprA* operon using BLASTn was performed, showing the presence of this operon in the *aeruginosa* and *paraeruginosa* species, two closely related species.

One of the most representative features of the *paraeruginosa* species is the presence of the *mexXY-oprA* operon, yet, the *oprA* gene has been shown to be shared between *P. paraeruginosa* and the outlier *P. aeruginosa* group where CMC-115 strain belongs (Déraspe et al., 2025).

Due to the species reclassification, phylogenetic analysis was carried out based on *rpoB* gene sequences. *rpoB* is a single-copy gene universally present in the bacterial kingdom; its high mutation rate makes it ideal for discrimination between closely related species rather than 16S rRNA gene (Bivand et al., 2024). This allowed us to confirm that most of the analysed strains in the study belonged to the *paraeruginosa* species; two of the analysed strains were confirmed to belong to the *aeruginosa* species, more closely related to PAO1 strain.

It was observed that the presence of the *mexXY-oprA* operon was mainly present in clinical isolates (Kavanaugh et al., 2025), but it can be found in *P. paraeruginosa* environmental isolates as well, contributing to multidrug resistance phenotypes.

Synteny analysis revealed a highly conserved *mexXY-oprA* operon, including upstream and downstream regions in the genome without integrase specific sites surrounding the operon of interest, supporting the theory of vertical gene transfer and evolution of the species. The main variation was the repressor *mexZ* located immediately upstream of the operon, which is of note as mutations in this gene can lead to the overexpression of the efflux pump (Morita et al., 2012b).

3.4. Conclusion and future directions

In conclusion, *mexXY-oprA* operon is predominantly present in *P. paraeruginosa*, although it is also present in a small number of *P. aeruginosa* clinical strains, which may be contributing to antibiotic resistance. The observed discrepancy between NCBI database annotation and *rpoB*-based phylogenetic classification could be misleading operon prevalence studies if these are based solely on database-derived taxonomy.

To expand the study of *mexXY-oprA* prevalence within *Pseudomonas* species, future work should focus on expanding the genomic samples including shotgun sequences and metagenomic datasets, to refine and detect diversity within the operon and genomic context. In addition, phylogenetic analysis of the *mexY* gene could provide a further insight to the evolutionary history of the *mexXY-oprA* operon providing hints of vertical inheritance or horizontal gene transfer when compared to the *rpoB* phylogenetic tree of this study. Finally, further analysis of the impact of the *mexZ* repressor variation across *P. paraeruginosa* strains may help to elucidate the impact of regulatory mechanisms influencing operon expression.

References

Aendekerk, S., Ghysels, B., Cornelis, P., & Baysse, C. (2002). Characterization of a new efflux pump, MexGHI-OpmD, from *Pseudomonas aeruginosa* that confers resistance to vanadium. *Microbiology (Reading, England)*, *148*(Pt 8), 2371–2381. https://doi.org/10.1099/00221287-148-8-2371

Akama, H., Kanemaki, M., Yoshimura, M., Tsukihara, T., Kashiwagi, T., Yoneyama, H., Narita, S. I., Nakagawa, A., & Nakae, T. (2004). Crystal structure of the drug discharge outer membrane protein, OprM, of *Pseudomonas aeruginosa*: Dual modes of membrane anchoring and occluded cavity end. *Journal of Biological Chemistry*, *279*(51), 52816–52819. https://doi.org/10.1074/jbc.C400445200

Alav, I., Kobylka, J., Kuth, M. S., Pos, K. M., Picard, M., Blair, J. M. A., & Bavro, V. N. (2021). Structure, Assembly, and Function of Tripartite Efflux and Type 1 Secretion Systems in Gram-Negative Bacteria. *Chemical Reviews*, *121*(9), 5479–5596. https://doi.org/10.1021/ACS.CHEMREV.1C00055

Asensio-Calavia, A., Ceballos-Munuera, Á., Méndez-Pérez, A., Álvarez, B., & Fernández, L. Á. (2024). A tuneable genetic switch for tight control of *tac* promoters in *Escherichia coli* boosts expression of synthetic injectisomes. *Microbial Biotechnology*, *17*(1), e14328. https://doi.org/10.1111/1751-7915.14328

Avakh, A., Grant, G. D., Cheesman, M. J., Kalkundri, T., & Hall, S. (2023). The Art of War with Pseudomonas aeruginosa: Targeting Mex Efflux Pumps Directly to Strategically Enhance Antipseudomonal Drug Efficacy. In *Antibiotics* (Vol. 12, Number 8). Multidisciplinary Digital Publishing Institute (MDPI). https://doi.org/10.3390/antibiotics12081304

Barry, A. L., Reller, L. B., Miller, G. H., Washington, J. A., Schoenknect, F. D., Peterson, L. R., Hare, R. S., & Knapp4, A. C. (1992). Revision of Standards for Adjusting the Cation Content of Mueller-Hinton Broth for Testing Susceptibility of *Pseudomonas aeruginosa* to Aminoglycosides. In *JOURNAL OF CLINICAL MICROBIOLOGY* (Vol. 30, Number 3). https://doi.org/10.1128/jcm.30.3.585-589.1992.

Bivand, J. M., Dyrhovden, R., Sivertsen, A., Tellevik, M. G., Patel, R., & Kommedal, Ø. (2024). Broad-range amplification and sequencing of the *rpoB* gene: a novel assay for bacterial identification in clinical microbiology. *Journal of Clinical Microbiology*, *62*(7). https://doi.org/10.1128/jcm.00266-24

Blair, J. M., & Piddock, L. J. (2009). Structure, function and inhibition of RND efflux pumps in Gram-negative bacteria: an update. *Current Opinion in Microbiology*, *12*(5), 512–519. https://doi.org/10.1016/J.MIB.2009.07.003

Breidenstein, E. B. M., de la Fuente-Núñez, C., & Hancock, R. E. W. (2011). *Pseudomonas aeruginosa*: all roads lead to resistance. *Trends in Microbiology*, *19*(8), 419–426. https://doi.org/10.1016/J.TIM.2011.04.005

Burmeister, A. R. (2015). Horizontal Gene Transfer. *Evolution, Medicine, and Public Health*, *2015*(1), 193–194. https://doi.org/10.1093/EMPH/EOV018

Castellani, C., & Assael, B. M. (2016). Cystic fibrosis: a clinical view. *Cellular and Molecular Life Sciences 2016 74:1*, *74*(1), 129–140. https://doi.org/10.1007/S00018-016-2393-9

CDC. (2025, January 31). *About Antimicrobial Resistance | Antimicrobial Resistance | CDC*. https://www.cdc.gov/antimicrobial-resistance/about/index.html

Choi, K. H., Gaynor, J. B., White, K. G., Lopez, C., Bosio, C. M., Karkhoff-Schweizer, R. A. R., & Schweizer, H. P. (2005). A Tn7-based broad-range bacterial cloning and expression system. *Nature Methods*, *2*(6), 443–448. https://doi.org/10.1038/nmeth765

Choi, K. H., & Schweizer, H. P. (2006). mini-Tn7 insertion in bacteria with single *att*Tn7 sites: Example *Pseudomonas aeruginosa*. *Nature Protocols*, *1*(1), 153–161. https://doi.org/10.1038/nprot.2006.24

Chuanchuen, R., Narasaki, C. T., & Schweizer, H. P. (2002). The MexJK Efflux Pump of *Pseudomonas aeruginosa* Requires OprM for Antibiotic Efflux but Not for Efflux of Triclosan. *Journal of Bacteriology*, *184*(18), 5036. https://doi.org/10.1128/JB.184.18.5036-5044.2002

Costa, O. Y. A., Raaijmakers, J. M., & Kuramae, E. E. (2018). Microbial extracellular polymeric substances: Ecological function and impact on soil aggregation. *Frontiers in Microbiology*, *9*(JUL), 337094. https://doi.org/10.3389/FMICB.2018.01636/FULL

Craig, N. L. (1991). Tn7: a target site-specific transposon. *Molecular Microbiology*, *5*(11), 2569–2573. https://doi.org/10.1111/J.1365-2958.1991.TB01964.X

Cystic Fibrosis Canada. (2024). *The Canadian Cystic Fibrosis Registry 2023 Annual Data report*. https://cysticfibrosis.ca/news/canadas-cystic-fibrosis-population-continues-to-grow

Déraspe, M., Burrows, L. L., Voulhoux, R., Centrón, D., Corbeil, J., & Roy, P. H. (2025). Comparative genomics of *Pseudomonas paraeruginosa*. *Journal of Bacteriology*, *207*(8). https://doi.org/10.1128/JB.00149-25;PAGE:STRING:ARTICLE/CHAPTER

Dong, N., Zeng, Y., Wang, Y., Liu, C., Lu, J., Cai, C., Liu, X., Chen, Y., Wu, Y., Fang, Y., Fu, Y., Hu, Y., Zhou, H., Cai, J., Hu, F., Wang, S., Wang, Y., Wu, Y., Chen, G., … Zhang, R. (2022). Distribution and spread of the mobilised RND efflux pump gene cluster *tmexCD-toprJ* in clinical Gram-negative bacteria: a molecular epidemiological study. *The Lancet Microbe*, *3*(11), e846–e856. https://doi.org/10.1016/S2666-5247(22)00221-X

Driscoll, J. A., Brody, S. L., & Kollef, M. H. (2007). The Epidemiology, Pathogenesis and Treatment of *Pseudomonas aeruginosa* Infections. In *Drugs* (Vol. 67, Number 3).

Du, D., Wang, Z., James, N. R., Voss, J. E., Klimont, E., Ohene-Agyei, T., Venter, H., Chiu, W., & Luisi, B. F. (2014). Structure of the AcrAB-TolC multidrug efflux pump. *Nature*, *509*(7501), 512. https://doi.org/10.1038/NATURE13205

Elfadadny, A., Ragab, R. F., AlHarbi, M., Badshah, F., Ibáñez-Arancibia, E., Farag, A., Hendawy, A. O., De los Ríos-Escalante, P. R., Aboubakr, M., Zakai, S. A., & Nageeb, W. M. (2024). Antimicrobial resistance of *Pseudomonas aeruginosa*: navigating clinical impacts, current resistance trends, and innovations in breaking therapies. *Frontiers in Microbiology*, *15*, 1374466. https://doi.org/10.3389/FMICB.2024.1374466/FULL

Habboush, Y., & Guzman, N. (2023). Antibiotic Resistance. *StatPearls*. https://www.ncbi.nlm.nih.gov/books/NBK513277/

Hancock, R. E. W., & Brinkman, F. S. L. (2002). Function of *Pseudomonas* porins in uptake and efflux. *Annual Review of Microbiology*, *56*(Volume 56, 2002), 17–38. https://doi.org/10.1146/ANNUREV.MICRO.56.012302.160310/CITE/REFWORKS

Hancock, R. E. W., & Speert, D. P. (2000). Antibiotic resistance in *Pseudomonas aeruginosa*: mechanisms and impact on treatment. *Drug Resistance Updates*, *3*(4), 247–255. https://doi.org/10.1054/DRUP.2000.0152

Hansen, C., & Skov, M. (2015). Evidence for the efficacy of aztreonam for inhalation solution in the management of *Pseudomonas aeruginosa* in patients with cystic fibrosis. *Therapeutic Advances in Respiratory Disease*, *9*(1), 16–21. https://doi.org/10.1177/1753465814561624;REQUESTEDJOURNAL:JOURNAL:TARA;PAGE:STRING:ARTICLE/CHAPTER

Hoang, T. T., Karkhoff-Schweizer, R. R., Kutchma, A. J., & Schweizer, H. P. (1998). A broad-host-range Flp-FRT recombination system for site-specific excision of chromosomally-located DNA sequences: application for isolation of unmarked *Pseudomonas aeruginosa* mutants. In *Gene* (Vol. 212).

HOLLOWAY, B. W. (1955). Genetic recombination in *Pseudomonas aeruginosa*. *Journal of General Microbiology*, *13*(3), 572–581. https://doi.org/10.1099/00221287-13-3-572

Huang, Y. W., Hu, R. M., & Yang, T. C. (2013). Role of the *pcm-tolCsm* operon in the multidrug resistance of *Stenotrophomonas maltophilia*. *Journal of Antimicrobial Chemotherapy*, *68*(9), 1987–1993. https://doi.org/10.1093/JAC/DKT148

Jurado-Martín, I., Sainz-Mejías, M., & McClean, S. (2021). *Pseudomonas aeruginosa*: An Audacious Pathogen with an Adaptable Arsenal of Virulence Factors. *International Journal of Molecular Sciences 2021, Vol. 22, Page 3128*, *22*(6), 3128. https://doi.org/10.3390/IJMS22063128

Kavanaugh, L. G., Hinrichsen, M. E., Dunham, C. M., & Conn, G. L. (2025). Regulation, structure, and activity of the *Pseudomonas aeruginosa* MexXY efflux system. *Antimicrobial Agents and Chemotherapy*, *69*(5). https://doi.org/10.1128/AAC.01825-24;ISSUE:ISSUE:DOI

Klockgether, J., Cramer, N., Wiehlmann, L., Davenport, C. F., & Tümmler, B. (2011). *Pseudomonas aeruginosa* genomic structure and diversity. *Frontiers in Microbiology*, *2*(JULY), 10805. https://doi.org/10.3389/fmicb.2011.00150

Köhler, T., Michéa-Hamzehpour, M., Henze, U., Gotoh, N., Curty, L. K., & Pechère, J. C. (1997). Characterization of MexE-MexF-OprN, a positively regulated multidrug efflux system of *Pseudomonas aeruginosa*. *Molecular Microbiology*, *23*(2), 345–354. https://doi.org/10.1046/J.1365-2958.1997.2281594.X

Koronakis, V., Sharff, A., Koronakis, E., Luisi, B., & Hughes, C. (2000). Crystal structure of the bacterial membrane protein TolC central to multidrug efflux and protein export. *Nature 2000 405:6789*, *405*(6789), 914–919. https://doi.org/10.1038/35016007

Krell, T., & Matilla, M. A. (2024). *Pseudomonas aeruginosa*. *Trends in Microbiology*, *32*(2), 216–218. https://doi.org/10.1016/j.tim.2023.11.005

Kumar, A., Chua, K. L., & Schweizer, H. P. (2006). Method for regulated expression of single-copy efflux pump genes in a surrogate *Pseudomonas aeruginosa* strain: identification of the BpeEF-OprC chloramphenicol and trimethoprim efflux pump

of *Burkholderia pseudomallei* 1026b. *Antimicrobial Agents and Chemotherapy*, *50*(10), 3460–3463. https://doi.org/10.1128/AAC.00440-06

Kumar, A., & Schweizer, H. P. (2005). Bacterial resistance to antibiotics: Active efflux and reduced uptake. *Advanced Drug Delivery Reviews*, *57*(10), 1486–1513. https://doi.org/10.1016/J.ADDR.2005.04.004

Kumar, S., Stecher, G., Suleski, M., Sanderford, M., Sharma, S., & Tamura, K. (2024). MEGA12: Molecular Evolutionary Genetic Analysis Version 12 for Adaptive and Green Computing. *Molecular Biology and Evolution*, *41*(12). https://doi.org/10.1093/molbev/msae263

Kyriacou, S. V., Nowak, M. E., Brownlow, W. J., & Xu, X.-H. N. (2002). Single live cell imaging for real-time monitoring of resistance mechanism in *Pseudomonas aeruginosa*. *Journal of Biomedical Optics*, *7*(4), 576. https://doi.org/10.1117/1.1506707

Langendonk, R. F., Neill, D. R., & Fothergill, J. L. (2021). The Building Blocks of Antimicrobial Resistance in *Pseudomonas aeruginosa*: Implications for Current Resistance-Breaking Therapies. *Frontiers in Cellular and Infection Microbiology*, *11*, 665759. https://doi.org/10.3389/FCIMB.2021.665759/FULL

Lei Dai, Z. S. E. W. Y. Q. Z. (2016). Efflux Pumps in Campylobacter: Key Players for Antimicrobial Resistance and Environmental Adaption. In *Efflux-Mediated Antimicrobial Resistance in Bacteria* (pp. 471–487).

Letizia, M., Diggle, S. P., & Whiteley, M. (2025). *Pseudomonas aeruginosa*: ecology, evolution, pathogenesis and antimicrobial susceptibility. *Nature Reviews Microbiology 2025*, 1–17. https://doi.org/10.1038/s41579-025-01193-8

Li, X. Z., Poole, K., & Nikaido, H. (2003). Contributions of MexAB-OprM and an EmrE homolog to intrinsic resistance of *Pseudomonas aeruginosa* to aminoglycosides and dyes. *Antimicrobial Agents and Chemotherapy*, *47*(1), 27–33. https://doi.org/10.1128/AAC.47.1.27-33.2003

Li, Y., Mima, T., Komori, Y., Morita, Y., Kuroda, T., Mizushima, T., & Tsuchiya, T. (2003). A new member of the tripartite multidrug efflux pumps, MexVW-OprM, in *Pseudomonas aeruginosa*. *The Journal of Antimicrobial Chemotherapy*, *52*(4), 572–575. https://doi.org/10.1093/JAC/DKG390

Lister, P. D., Wolter, D. J., & Hanson, N. D. (2009). Antibacterial-resistant *Pseudomonas aeruginosa*: Clinical impact and complex regulation of chromosomally encoded

resistance mechanisms. *Clinical Microbiology Reviews*, *22*(4), 582–610. https://doi.org/10.1128/CMR.00040-09/FORMAT/EPUB

Ludovico, A., Moran, O., & Baroni, D. (2022). Modulator Combination Improves In Vitro the Microrheological Properties of the Airway Surface Liquid of Cystic Fibrosis Airway Epithelia. *International Journal of Molecular Sciences*, *23*(19), 11396. https://doi.org/10.3390/IJMS231911396/S1

Lund-Palau, H., Turnbull, A. R., Bush, A., Bardin, E., Cameron, L., Soren, O., Wierre-Gore, N., Alton, E. W. F. W., Bundy, J. G., Connett, G., Faust, S. N., Filloux, A., Freemont, P., Jones, A., Khoo, V., Morales, S., Murphy, R., Pabary, R., Simbo, A., … Davies, J. C. (2016). *Pseudomonas aeruginosa* infection in cystic fibrosis: pathophysiological mechanisms and therapeutic approaches. *Expert Review of Respiratory Medicine*, *10*(6), 685–697. https://doi.org/10.1080/17476348.2016.1177460

Ma, D., Cook, D. N., Alberti, M., Pon, N. G., Nikaido, H., & Hearst, J. E. (1993). Molecular cloning and characterization of *acrA* and *acrE* genes of *Escherichia coli*. *Journal of Bacteriology*, *175*(19), 6299–6313. https://doi.org/10.1128/JB.175.19.6299-6313.1993

Masi, M., & Pagès, J.-M. (2013). Structure, Function and Regulation of Outer Membrane Proteins Involved in Drug Transport in Enterobactericeae: the OmpF/C – TolC Case. *The Open Microbiology Journal*, *7*(1), 22. https://doi.org/10.2174/1874285801307010022

Mima, T., Joshi, S., Gomez-Escalada, M., & Schweizer, H. P. (2007). Identification and Characterization of TriABC-OpmH, a Triclosan Efflux Pump of *Pseudomonas aeruginosa* Requiring Two Membrane Fusion Proteins. *Journal of Bacteriology*, *189*(21), 7600. https://doi.org/10.1128/JB.00850-07

Mima, T., Kohira, N., Li, Y., Sekiya, H., Ogawa, W., Kuroda, T., & Tsuchiya, T. (2009). Gene cloning and characteristics of the RND-type multidrug efflux pump MuxABC-OpmB possessing two RND components in *Pseudomonas aeruginosa*. *Microbiology (Reading, England)*, *155*(Pt 11), 3509–3517. https://doi.org/10.1099/MIC.0.031260-0

Mima, T., Sekiya, H., Mizushima, T., Kuroda, T., & Tsuchiya, T. (2005). Gene cloning and properties of the RND-type multidrug efflux pumps MexPQ-OpmE and MexMN-OprM from *Pseudomonas aeruginosa*. *Microbiology and Immunology*, *49*(11), 999–1002. https://doi.org/10.1111/J.1348-0421.2005.TB03696.X

Mine, T., Morita, Y., Kataoka, A., Mizushima, T., & Tsuchiya, T. (1999). Expression in *Escherichia coli* of a new multidrug efflux pump, MexXY, from *Pseudomonas aeruginosa*. *Antimicrobial Agents and Chemotherapy*, *43*(2), 415–417. https://doi.org/10.1128/AAC.43.2.415

Miranda, S. W., Asfahl, K. L., Dandekar, A. A., & Greenberg, E. P. (2022). *Pseudomonas aeruginosa* Quorum Sensing. *Advances in Experimental Medicine and Biology*, *1386*, 95. https://doi.org/10.1007/978-3-031-08491-1_4

Mirdita, M., Schütze, K., Moriwaki, Y., Heo, L., Ovchinnikov, S., & Steinegger, M. (2022). ColabFold: making protein folding accessible to all. *Nature Methods 2022 19:6*, *19*(6), 679–682. https://doi.org/10.1038/s41592-022-01488-1

Moradali, M. F., Ghods, S., & Rehm, B. H. A. (2017). *Pseudomonas aeruginosa* lifestyle: A paradigm for adaptation, survival, and persistence. *Frontiers in Cellular and Infection Microbiology*, *7*(FEB), 249785. https://doi.org/10.3389/FCIMB.2017.00039/FULL

Morita, Y., Tomida, J., & Kawamura, Y. (2012a). Mexxy multidrug efflux system of *Pseudomonas aeruginosa*. *Frontiers in Microbiology*, *3*(NOV), 38395. https://doi.org/10.3389/FMICB.2012.00408/FULL

Morita, Y., Tomida, J., & Kawamura, Y. (2012b). Primary mechanisms mediating aminoglycoside resistance in the multidrug-resistant *Pseudomonas aeruginosa* clinical isolate PA7. *Microbiology*, *158*(4), 1071–1083. https://doi.org/10.1099/mic.0.054320-0

Murakami, S., Nakashima, R., Yamashita, E., Matsumoto, T., & Yamaguchi, A. (2006). Crystal structures of a multidrug transporter reveal a functionally rotating mechanism. *Nature 2006 443:7108*, *443*(7108), 173–179. https://doi.org/10.1038/nature05076

Nehme, D., & Poole, K. (2007). Assembly of the MexAB-OprM Multidrug Pump of *Pseudomonas aeruginosa*: Component Interactions Defined by the Study of Pump Mutant Suppressors. *Journal of Bacteriology*, *189*(17), 6118. https://doi.org/10.1128/JB.00718-07

Nikaido, H. (2011). STRUCTURE AND MECHANISM OF RND-TYPE MULTIDRUG EFFLUX PUMPS. *Advances in Enzymology and Related Areas of Molecular Biology*, *77*, 1. https://doi.org/10.1002/9780470920541.CH1

Oakland, M., Sinn, P. L., & McCray, P. B. (2012). Advances in Cell and Gene-based Therapies for Cystic Fibrosis Lung Disease. *Molecular Therapy*, *20*(6), 1108–1115. https://doi.org/10.1038/MT.2012.32

Pang, Z., Raudonis, R., Glick, B. R., Lin, T. J., & Cheng, Z. (2019). Antibiotic resistance in *Pseudomonas aeruginosa*: mechanisms and alternative therapeutic strategies. In *Biotechnology Advances* (Vol. 37, Number 1, pp. 177–192). Elsevier Inc. https://doi.org/10.1016/j.biotechadv.2018.11.013

Phan, G., Benabdelhak, H., Lascombe, M. B., Benas, P., Rety, S., Picard, M., Ducruix, A., Etchebest, C., & Broutin, I. (2010). Structural and Dynamical Insights into the Opening Mechanism of *P. aeruginosa* OprM Channel. *Structure*, *18*(4), 507–517. https://doi.org/10.1016/j.str.2010.01.018

Phan, G., Picard, M., & Broutin, I. (2015). Focus on the Outer Membrane Factor OprM, the Forgotten Player from Efflux Pumps Assemblies. *Antibiotics 2015, Vol. 4, Pages 544-566*, *4*(4), 544–566. https://doi.org/10.3390/ANTIBIOTICS4040544

Poole, K., Gotoh, N., Tsujimoto, H., Zhao, Q., Wada, A., Yamasaki, T., Neshat, S., Yamagishi, J. I., Li, X. Z., & Nishino, T. (1996). Overexpression of the *mexC-mexD-oprJ* efflux operon in *nfxB*-type multidrug-resistant strains of *Pseudomonas aeruginosa*. *Molecular Microbiology*, *21*(4), 713–725. https://doi.org/10.1046/J.1365-2958.1996.281397.X;SUBPAGE:STRING:ABSTRACT;WEBSITE:WEBSITE:PERICLES;JOURNAL:JOURNAL:13652958;WGROUP:STRING:PUBLICATION

Poole, K., Krebes, K., McNally, C., & Neshat, S. (1993). Multiple antibiotic resistance in *Pseudomonas aeruginosa*: evidence for involvement of an efflux operon. *Journal of Bacteriology*, *175*(22), 7363–7372. https://doi.org/10.1128/JB.175.22.7363-7372.1993

Poole, K., & Srikumar, R. (2001). Multidrug Efflux in *Pseudomonas aeruginosa*: Components, Mechanisms and Clinical Significance. In *Current Topics in Medicinal Chemistry* (Vol. 1). http://www.pseudomonas.com/

Riordan, J. R. (2005). Assembly of functional CFTR chloride channels. *Annual Review of Physiology*, *67*, 701–718. https://doi.org/10.1146/annurev.physiol.67.032003.154107

Ropy, A., Cabot, G., Sánchez-Diener, I., Aguilera, C., Moya, B., Ayala, J. A., & Oliver, A. (2015). Role of *Pseudomonas aeruginosa* low-molecular-mass penicillin-binding proteins in AmpC expression, β-lactam resistance, and peptidoglycan structure.

Antimicrobial Agents and Chemotherapy, *59*(7), 3925–3934. https://doi.org/10.1128/AAC.05150-14;WGROUP:STRING:PUBLICATION

Rossi, E., La Rosa, R., Bartell, J. A., Marvig, R. L., Haagensen, J. A. J., Sommer, L. M., Molin, S., & Johansen, H. K. (2020). *Pseudomonas aeruginosa* adaptation and evolution in patients with cystic fibrosis. *Nature Reviews Microbiology 2020 19:5*, *19*(5), 331–342. https://doi.org/10.1038/s41579-020-00477-5

Roy, P. H., Tetu, S. G., Larouche, A., Elbourne, L., Tremblay, S., Ren, Q., Dodson, R., Harkins, D., Shay, R., Watkins, K., Mahamoud, Y., & Paulsen, I. T. (2010). Complete genome sequence of the multiresistant taxonomic outlier *Pseudomonas aeruginosa* PA7. *PloS One*, *5*(1). https://doi.org/10.1371/JOURNAL.PONE.0008842

Rudra, B., Duncan, L., Shah, A. J., Shah, H. N., & Gupta, R. S. (2022). Phylogenomic and comparative genomic studies robustly demarcate two distinct clades of *Pseudomonas aeruginosa* strains: proposal to transfer the strains from an outlier clade to a novel species *Pseudomonas paraeruginosa* sp. nov. *International Journal of Systematic and Evolutionary Microbiology*, *72*(11). https://doi.org/10.1099/ijsem.0.005542

Rutherford, S. T., & Bassler, B. L. (2012). Bacterial Quorum Sensing: Its Role in Virulence and Possibilities for Its Control. *Cold Spring Harbor Perspectives in Medicine*, *2*(11), a012427. https://doi.org/10.1101/CSHPERSPECT.A012427

Satoshi Murakami. (2016). Structures and Transport Mechanisms of RND Efflux Pumps. In *Bacterial Drug Efflux Pumps: Structures and Transport Mechanisms* (pp. 3–28).

Schroeter, J. (1872). Ueber einige durch Bacterien gebildete Pigmente. *Beiträge Zur Biologie Der Pflanzen*, *1*(2), 109–126.

Schuster, M., & Greenberg, E. P. (2006). A network of networks: Quorum-sensing gene regulation in *Pseudomonas aeruginosa*. *International Journal of Medical Microbiology*, *296*(2–3), 73–81. https://doi.org/10.1016/J.IJMM.2006.01.036

Singh, M., Sykes, E. M. E., Li, Y., & Kumar, A. (2020). MexXY RND pump of *Pseudomonas aeruginosa* PA7 effluxes bi-anionic β-lactams carbenicillin and sulbenicillin when it partners with the outer membrane factor OprA but not with OprM. *Microbiology (United Kingdom)*, *166*(11), 1095–1106. https://doi.org/10.1099/mic.0.000971

Stover, C. K., Pham, X. Q., Erwin, A. L., Mizoguchi, S. D., Warrener, P., Hickey, M. J., Brinkman, F. S. L., Hufnagle, W. O., Kowallk, D. J., Lagrou, M., Garber, R. L., Goltry, L., Tolentino, E., Westbrock-Wadman, S., Yuan, Y., Brody, L. L., Coulter, S. N., Folger, K. R., Kas, A., … Olson, M. V. (2000). Complete genome sequence of *Pseudomonas aeruginosa* PAO1, an opportunistic pathogen. *Nature*, *406*(6799), 959–964. https://doi.org/10.1038/35023079

Symmons, M. F., Bokma, E., Koronakis, E., Hughes, C., & Koronakis, V. (2009). The assembled structure of a complete tripartite bacterial multidrug efflux pump. *Proceedings of the National Academy of Sciences of the United States of America*, *106*(17), 7173–7178. https://doi.org/10.1073/PNAS.0900693106;WEBSITE:WEBSITE:PNAS-SITE;WGROUP:STRING:PUBLICATION

Urban-Chmiel, R., Marek, A., Stępień-Pyśniak, D., Wieczorek, K., Dec, M., Nowaczek, A., & Osek, J. (2022). Antibiotic Resistance in Bacteria—A Review. *Antibiotics*, *11*(8), 1079. https://doi.org/10.3390/ANTIBIOTICS11081079/S1

van den Belt, M., Gilchrist, C., Booth, T. J., Chooi, Y. H., Medema, M. H., & Alanjary, M. (2023). CAGECAT: The CompArative GEne Cluster Analysis Toolbox for rapid search and visualisation of homologous gene clusters. *BMC Bioinformatics*, *24*(1), 181. https://doi.org/10.1186/S12859-023-05311-2

Vettoretti, L., Plésiat, P., Muller, C., El Garch, F., Phan, G., Attrée, I., Ducruix, A., & Llanes, C. (2009). Efflux Unbalance in *Pseudomonas aeruginosa* Isolates from Cystic Fibrosis Patients. *Antimicrobial Agents and Chemotherapy*, *53*(5), 1987. https://doi.org/10.1128/AAC.01024-08

Weinstein, M. P. . (2018). *Methods for dilution antimicrobial susceptibility tests for bacteria that grow aerobically*. Clinical Laboratory Standards Institute.

World Health Organization. (2024). WHO Bacterial Priority Pathogens List, 2024-Bacterial pathogens of public health importance to guide research, development and strategies to prevent and control antimicrobial resistance. *World Health Organization*, 1–72. https://iris.who.int/bitstream/handle/10665/376776/9789240093461-eng.pdf

Yamanaka, H., Tadokoro, S., Miyano, M., Takahashi, E., Kobayashi, H., & Okamoto, K. (2007). Studies on the region involved in the transport activity of *Escherichia coli* TolC by chimeric protein analysis. *Microbial Pathogenesis*, *42*, 184–192. https://doi.org/10.1016/j.micpath.2007.01.006

Yoshihara, E., Eda, S., & Kaitou, S. (2009). Functional interaction sites of OprM with MexAB in the *Pseudomonas aeruginosa* multidrug efflux pump. *FEMS Microbiology Letters*, *299*(2), 200–204. https://doi.org/10.1111/j.1574-6968.2009.01752.x

Zhang, Z., Schwartz, S., Wagner, L., & Miller, W. (2000). A greedy algorithm for aligning DNA sequences. *Journal of Computational Biology : A Journal of Computational Molecular Cell Biology*, *7*(1–2), 203–214. https://doi.org/10.1089/10665270050081478

Appendices

Appendix 1. Gibson assembly reaction mix

Component	Amount
MiniTn7-*mexXY* backbone	0.050 pmoles (X µl)
oprM/oprA mutant fragment	0.100 pmoles (Y µl)
Gibson Assembly master mix	10.0 µl
Deionized H_2O	10-X-Y µl
Total volume	20 µl

Appendix 2. PCR reaction and thermal cycling parameters pUC18-mini-Tn7T-Lac-Gm-*mexXY.*

PCR reaction mix

5x VeriFi Buffer	5 µl
10x VeriMax enhancer	2.5 µl
Forward primer (10 µM)	1 µl
Reverse primer (10 µM)	1 µl
Template DNA	10 ng
VeriFi polymerase	0.25 µl
H_2O	up to 25 µl

Thermal cycle conditions

	98°C	1 min
35x	98°C	15 seg
	65°C	30 seg
	75°C	8 min 30 seg
	75°C	5 min
	4°C	On hold

Appendix 3. PCR reaction and thermal cycling parameters *oprM/oprA* fragments.

PCR reaction mix

5x VeriFi Buffer	5 µl
10x VeriMax enhancer	2.5 µl
Forward primer (10 µM)	1 µl
Reverse primer (10 µM)	1 µl
Template DNA	20 ng
VeriFi polymerase	0.25 µl
H_2O	up to 25 µl

Thermal cycle conditions

	98°C	1 min
35x	98°C	15 seg
	63°C	30 seg
	75°C	45 seg
	75°C	5 min
	4°C	On hold

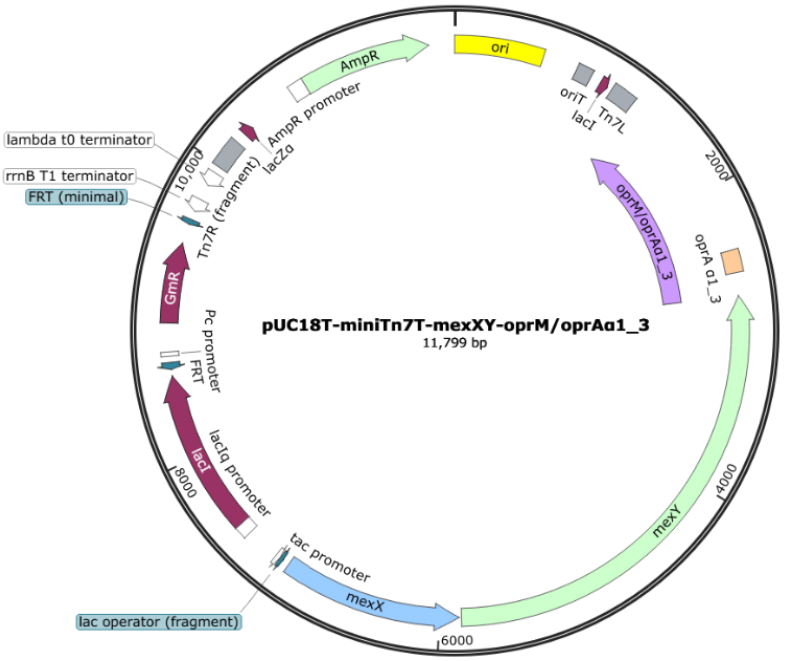

Appendix 4. Secuenced plasmid pUC18-Mini-Tn7T-Gm-Lac-*mexXY-oprM/oprAα1_3*. Plasmid maps generated via whole plasmid sequencing (Plasmidsaurus) Image created with SnapGene version 8.2.2. Orange feature in plasmid shows *oprA* fraction in the *oprM/oprA* chimera gene.

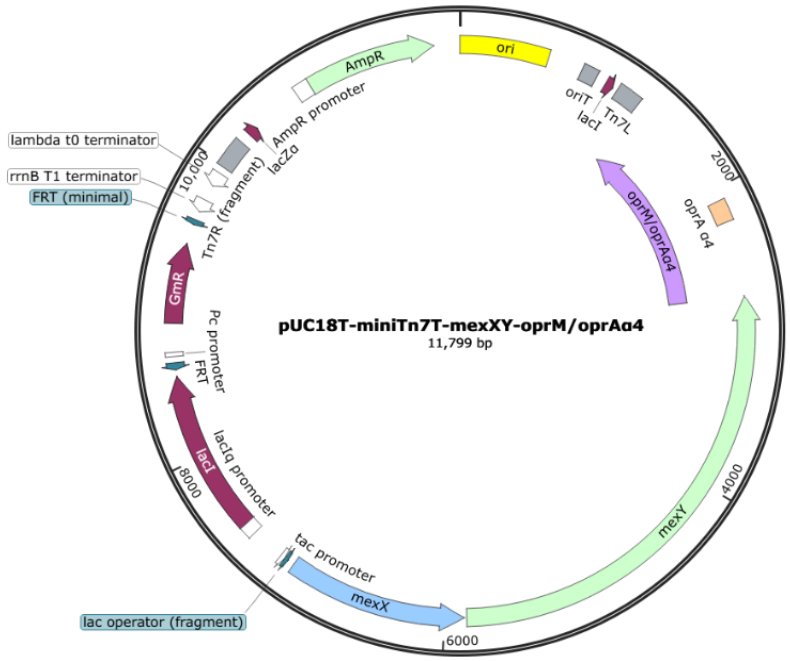

Appendix 5. Secuenced plasmid pUC18-Mini-Tn7T-Gm-Lac-*mexXY-oprM/oprAα4*. Plasmid maps generated via whole plasmid sequencing (Plasmidsaurus) Image created with SnapGene version 8.2.2. Orange feature in plasmid shows *oprA* fraction in the *oprM/oprA* chimera gene.

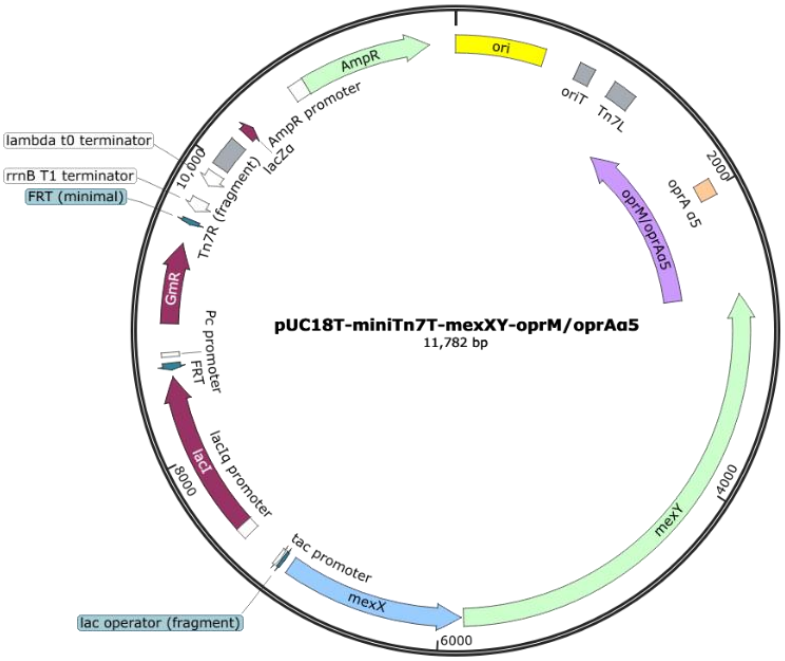

Appendix 6. Secuenced plasmid pUC18-Mini-Tn7T-Gm-Lac-*mexXY-oprM/oprAα4*. Plasmid maps generated via whole plasmid sequencing (Plasmidsaurus) Image created with SnapGene version 8.2.2. Orange feature in plasmid shows *oprA* fraction in the *oprM/oprA* chimera gene.

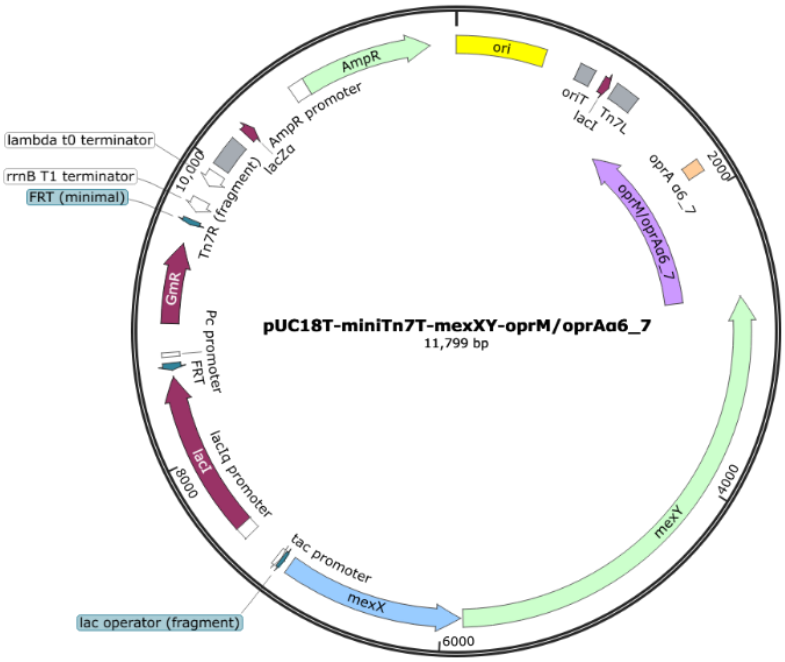

Appendix 7. Secuenced plasmid pUC18-Mini-Tn7T-Gm-Lac-*mexXY-oprM/oprAα6_7*. Plasmid maps generated via whole plasmid sequencing (Plasmidsaurus) Image created with SnapGene version 8.2.2. Orange feature in plasmid shows *oprA* fraction in the *oprM/oprA* chimera gene.

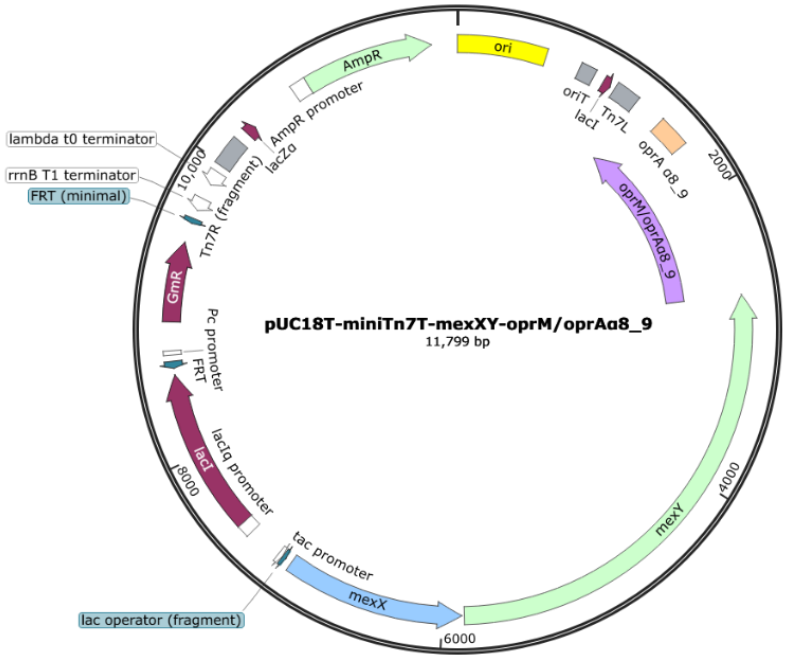

Appendix 8. Secuenced plasmid pUC18-Mini-Tn7T-Gm-Lac-*mexXY-oprM/oprAα8_9*. Plasmid maps generated via whole plasmid sequencing (Plasmidsaurus) Image created with SnapGene version 8.2.2. Orange feature in plasmid shows *oprA* fraction in the *oprM/oprA* chimera gene.

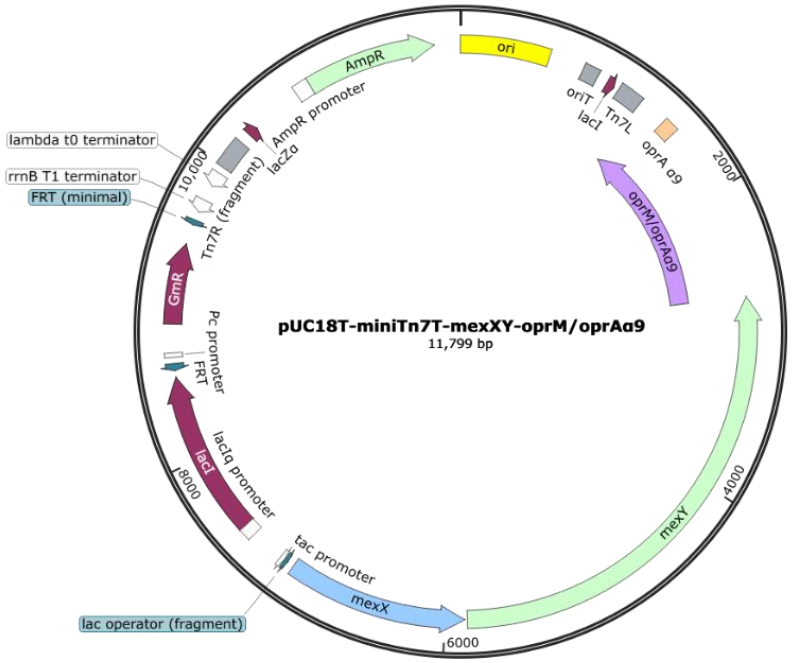

Appendix 9. Secuenced plasmid pUC18-Mini-Tn7T-Gm-Lac-*mexXY-oprM/oprAα9*. Plasmid maps generated via whole plasmid sequencing (Plasmidsaurus) Image created with SnapGene version 8.2.2. Orange feature in plasmid shows *oprA* fraction in the *oprM/oprA* chimera gene.

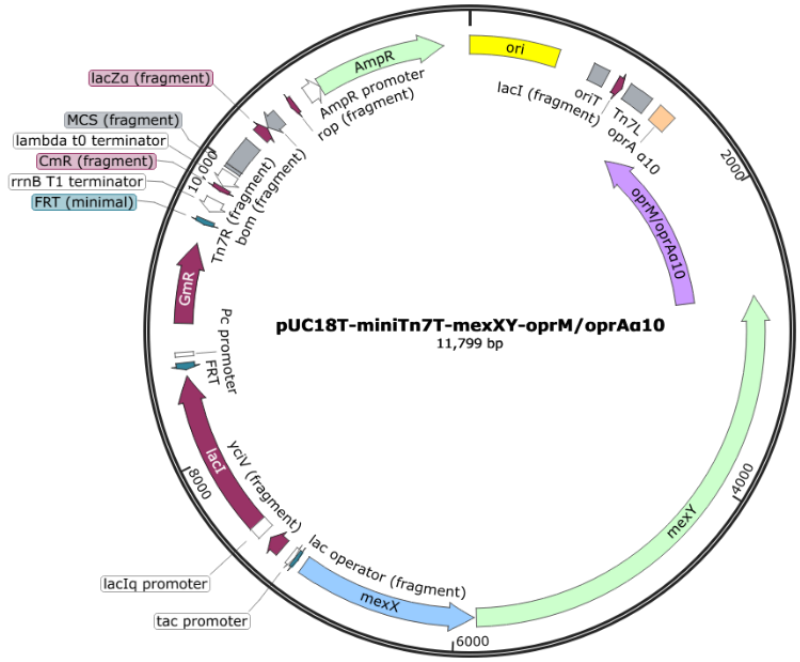

Appendix 10. Secuenced plasmid pUC18-Mini-Tn7T-Gm-Lac-*mexXY-oprM/oprAα10*. Plasmid maps generated via whole plasmid sequencing (Plasmidsaurus) Image created with SnapGene version 8.2.2. Orange feature in plasmid shows *oprA* fraction in the *oprM/oprA* chimera gene.